

Polarized forward–backward asymmetries of leptons in

$$B_s \rightarrow \ell^+ \ell^- \gamma \text{ decay}$$

T. M. Aliev ^{*}, V. Bashiry [†], M. Savci [‡]

Physics Department, Middle East Technical University, 06531 Ankara, Turkey

Abstract

Polarized forward–backward asymmetries in the $B_s \rightarrow \ell^+ \ell^- \gamma$ decay are calculated using the most general, model independent form of the effective Hamiltonian, including all possible forms of interactions. The dependencies of the asymmetries on new Wilson coefficients are investigated. The detectability of the asymmetries at LHC is discussed.

PACS numbers: 12.60.–i, 13.30.–a

^{*}e-mail: taliev@metu.edu

[†]e-mail: bashiry@newton.physics.metu.edu.tr

[‡]e-mail: savci@metu.edu

1 Introduction

Rare radiative leptonic $B_{s(d)} \rightarrow \ell^+ \ell^- \gamma$ decays are induced by the flavor-changing neutral current transitions $b \rightarrow s(d)$. In the standard model (SM) such processes are described by the penguin and box diagrams and have branching ratios $10^{-8} - 10^{-15}$ (see for example [1]). These rare decays can not be observed at the running machines such as Tevatron, BaBar and Belle, but the $B_{s(d)} \rightarrow \mu^+ \mu^-$ and $B_{s(d)} \rightarrow \mu^+ \mu^- \gamma$ decays can be detected at LHC with ATLAS, CMS and LHCb detectors [2]. Many experimental observables such as, the branching ratio, photon energy, dilepton mass spectra and charge asymmetries, as well as the transition form factors, are investigated for the $B_{s(d)} \rightarrow \ell^+ \ell^- \gamma$ decays in [3–9]. At the same time $B_{s(d)} \rightarrow \ell^+ \ell^- \gamma$ decays might be sensitive to the new physics beyond the SM. New physics effects in these decays can appear in two different ways: either through the new operators in the effective Hamiltonian which are absent in the SM, or through new contributions to the Wilson coefficients existing in the SM. One efficient way for precise determination of the SM parameters and looking for new physics beyond the SM is studying the lepton polarization effects. It has been pointed out in [10] that some of the single lepton polarization asymmetries might be too small to be observed and might not provide sufficient number of observables in checking the structure of the effective Hamiltonian. In need of more observables, in [10], the maximum number of independent observables have been constructed by considering the situation where both lepton polarizations are simultaneously measured.

In the present work, we analyze the possibility of searching for new physics in the $B_s \rightarrow \ell^+ \ell^- \gamma$ decay by studying the forward-backward asymmetries when both leptons are polarized, using the most general, model independent form of the effective Hamiltonian including all possible interactions. Note that the sensitivity of double-lepton polarization asymmetries on new Wilson coefficients for the $B_s \rightarrow \ell^+ \ell^- \gamma$ decay has been investigated recently in [11].

The work is organized as follows. In section 2, the matrix element for the $B_s \rightarrow \ell^+ \ell^- \gamma$ is obtained, using the general, model independent form of the effective Hamiltonian. In section 3, we calculate the polarized forward-backward asymmetries of the leptons in $B_s \rightarrow \ell^+ \ell^- \gamma$ decay. Section 4 is devoted to the numerical analysis, discussions and conclusions.

2 Theoretical framework

In the present section we derive the matrix element for the $B_s \rightarrow \ell^+ \ell^- \gamma$ using the general, model independent form of the effective Hamiltonian. The matrix element for the process $B_s \rightarrow \ell^+ \ell^- \gamma$ can be obtained from that of the purely leptonic $B_s \rightarrow \ell^+ \ell^-$ decay. At inclusive level the process $B_s \rightarrow \ell^+ \ell^-$ is described by $b \rightarrow q \ell^+ \ell^-$ transition. The effective $b \rightarrow q \ell^+ \ell^-$ transition can be written in terms of twelve model independent four-Fermi interactions in the following form [12]:

$$\begin{aligned} \mathcal{H}_{eff} = & \frac{G\alpha}{\sqrt{2}\pi} V_{tq} V_{tb}^* \left\{ C_{SL} \bar{q} i \sigma_{\mu\nu} \frac{q^\nu}{q^2} L b \bar{\ell} \gamma^\mu \ell + C_{BR} \bar{q} i \sigma_{\mu\nu} \frac{q^\nu}{q^2} R b \bar{\ell} \gamma^\mu \ell \right. \\ & \left. + C_{LL}^{tot} \bar{q} \gamma_\mu L b \bar{\ell} \gamma^\mu L \ell + C_{LR}^{tot} \bar{q} \gamma_\mu L b \bar{\ell} \gamma^\mu R \ell + C_{RL} \bar{q} \gamma_\mu R b \bar{\ell} \gamma^\mu L \ell \right. \end{aligned}$$

$$\begin{aligned}
& + C_{RR} \bar{q} \gamma_\mu R b \bar{\ell} \gamma^\mu R \ell + C_{LRLR} \bar{q} R b \bar{\ell} R \ell + C_{RLLR} \bar{q} L b \bar{\ell} R \ell + C_{LRRL} \bar{q} R b \bar{\ell} L \ell \\
& + C_{RLRL} \bar{q} L b \bar{\ell} L \ell + C_T \bar{q} \sigma_{\mu\nu} b \bar{\ell} \sigma^{\mu\nu} \ell + i C_{TE} \epsilon^{\mu\nu\alpha\beta} \bar{q} \sigma_{\mu\nu} b \bar{\ell} \sigma_{\alpha\beta} \ell \Big\} , \tag{1}
\end{aligned}$$

where C_X are the coefficients of the four-Fermi interactions and

$$L = \frac{1 - \gamma_5}{2} , \quad R = \frac{1 + \gamma_5}{2} .$$

The terms with coefficients C_{SL} and C_{BR} which describe penguin contributions correspond to $-2m_s C_7^{eff}$ and $-2m_b C_7^{eff}$ in the SM, respectively. The next four terms in this expression are the vector interactions. The interaction terms containing C_{LL}^{tot} and C_{LR}^{tot} in the SM have the form $C_9^{eff} - C_{10}$ and $C_9^{eff} + C_{10}$, respectively. Inspired by this C_{LL}^{tot} and C_{LR}^{tot} will be written as

$$\begin{aligned}
C_{LL}^{tot} &= C_9^{eff} - C_{10} + C_{LL} , \\
C_{LR}^{tot} &= C_9^{eff} + C_{10} + C_{LR} ,
\end{aligned}$$

where C_{LL} and C_{LR} describe contributions from new physics. The terms with coefficients C_{LRLR} , C_{RLLR} , C_{LRRL} and C_{RLRL} describe the scalar type interactions. The last two terms in Eq. (1) with the coefficients C_T and C_{TE} describe the tensor type interactions.

Having presented the general form of the effective Hamiltonian the next problem is the calculation of the matrix element of the $B_q \rightarrow \ell^+ \ell^- \gamma$ decay. This matrix element can be written as the sum of the two parts, structure-dependent and inner-Bremsstrahlung parts

$$\mathcal{M} = \mathcal{M}_{SD} + \mathcal{M}_{IB} . \tag{2}$$

The matrix element for the structure-dependent part \mathcal{M}_{SD} , which corresponds to the radiation of photon from initial quarks, can be obtained by calculating the matrix element $\langle \gamma | \mathcal{H}_{eff} | B \rangle$. Using Eq. (1) we see that, for calculation of \mathcal{M}_{SD} , we need to know the following matrix elements

$$\begin{aligned}
& \langle \gamma | \bar{s} \gamma_\mu (1 \mp \gamma_5) b | B \rangle , \\
& \langle \gamma | \bar{s} \sigma_{\mu\nu} q^\nu b | B \rangle , \\
& \langle \gamma | \bar{s} \sigma_{\mu\nu} b | B \rangle , \\
& \langle \gamma | \bar{s} (1 \mp \gamma_5) b | B \rangle .
\end{aligned} \tag{3}$$

The first two of the matrix elements in Eq. (3) are defined in the following way [3, 7, 13, 14]

$$\langle \gamma(k) | \bar{q} \gamma_\mu (1 \mp \gamma_5) b | B(p_B) \rangle = \frac{e}{m_B^2} \left\{ \epsilon_{\mu\nu\lambda\sigma} \varepsilon^{*\nu} q^\lambda k^\sigma g(q^2) \pm i \left[\varepsilon^{*\mu}(kq) - (\varepsilon^* q) k^\mu \right] f(q^2) \right\} , \tag{4}$$

$$\langle \gamma(k) | \bar{q} \sigma_{\mu\nu} b | B(p_B) \rangle = \frac{e}{m_B^2} \epsilon_{\mu\nu\lambda\sigma} \left[G \varepsilon^{*\lambda} k^\sigma + H \varepsilon^{*\lambda} q^\sigma + N (\varepsilon^* q) q^\lambda k^\sigma \right] . \tag{5}$$

Here, ε^* and k are the four vector polarization and momentum of the photon, respectively, $q = p_B - k$ is the momentum transfer, p_B is the momentum of the B meson and $g(q^2)$,

$f(q^2)$, $G(q^2)$, $H(q^2)$ and $N(q^2)$ are the $B_s \rightarrow \gamma$ transition form factors. The matrix element $\langle \gamma(k) | \bar{s} \sigma_{\mu\nu} \gamma_5 b | B(p_B) \rangle$ can be obtained from Eq. (5) using the identity

$$\sigma_{\mu\nu} = -\frac{i}{2} \epsilon_{\mu\nu\alpha\beta} \sigma^{\alpha\beta} \gamma_5 .$$

The matrix elements $\langle \gamma(k) | \bar{s}(1 \mp \gamma_5)b | B(p_B) \rangle$ and $\langle \gamma | \bar{s} i \sigma_{\mu\nu} q^\nu b | B \rangle$ can be obtained from Eqs. (4) and (5) by multiplying them q^μ and q^ν , respectively, as a result of which we get

$$\langle \gamma(k) | \bar{s}(1 \mp \gamma_5)b | B(p_B) \rangle = 0 , \quad (6)$$

$$\langle \gamma | \bar{s} i \sigma_{\mu\nu} q^\nu b | B \rangle = \frac{e}{m_B^2} i \epsilon_{\mu\nu\alpha\beta} q^\nu \varepsilon^{\alpha*} k^\beta G . \quad (7)$$

The matrix element $\langle \gamma | \bar{s} i \sigma_{\mu\nu} q^\nu (1 + \gamma_5) b | B \rangle$ can be written in terms of the two form factors $f_1(q^2)$ and $g_1(q^2)$ that are calculated in the framework of QCD sum rules [3, 13] in the following way

$$\langle \gamma | \bar{s} i \sigma_{\mu\nu} q^\nu (1 + \gamma_5) b | B \rangle = \frac{e}{m_B^2} \left\{ \epsilon_{\mu\alpha\beta\sigma} \varepsilon^{\alpha*} q^\beta k^\sigma g_1(q^2) + i \left[\varepsilon_\mu^*(qk) - (\varepsilon^* q) k_\mu \right] f_1(q^2) \right\} . \quad (8)$$

It should be noted that these form factors were calculated in framework of the light-front model in [14]. Eqs. (5), (7) and (8) allow us to express G , H and N in terms of f_1 and g_1 . Eqs. (4)–(8) help us rewrite \mathcal{M}_{SD} in the following form

$$\begin{aligned} \mathcal{M}_{SD} = & \frac{\alpha G_F}{4\sqrt{2}\pi} V_{tb} V_{tq}^* \frac{e}{m_B^2} \left\{ \bar{\ell} \gamma^\mu (1 - \gamma_5) \ell \left[A_1 \epsilon_{\mu\nu\alpha\beta} \varepsilon^{*\nu} q^\alpha k^\beta + i A_2 \left(\varepsilon_\mu^*(kq) - (\varepsilon^* q) k_\mu \right) \right] \right. \\ & + \bar{\ell} \gamma^\mu (1 + \gamma_5) \ell \left[B_1 \epsilon_{\mu\nu\alpha\beta} \varepsilon^{*\nu} q^\alpha k^\beta + i B_2 \left(\varepsilon_\mu^*(kq) - (\varepsilon^* q) k_\mu \right) \right] \\ & + i \epsilon_{\mu\nu\alpha\beta} \bar{\ell} \sigma^{\mu\nu} \ell \left[G \varepsilon^{*\alpha} k^\beta + H \varepsilon^{*\alpha} q^\beta + N (\varepsilon^* q) q^\alpha k^\beta \right] \\ & \left. + i \bar{\ell} \sigma_{\mu\nu} \ell \left[G_1 (\varepsilon^{*\mu} k^\nu - \varepsilon^{*\nu} k^\mu) + H_1 (\varepsilon^{*\mu} q^\nu - \varepsilon^{*\nu} q^\mu) + N_1 (\varepsilon^* q) (q^\mu k^\nu - q^\nu k^\mu) \right] \right\} , \quad (9) \end{aligned}$$

where

$$\begin{aligned} A_1 &= \frac{1}{q^2} (C_{BR} + C_{SL}) g_1 + (C_{LL}^{tot} + C_{RL}) g , \\ A_2 &= \frac{1}{q^2} (C_{BR} - C_{SL}) f_1 + (C_{LL}^{tot} - C_{RL}) f , \\ B_1 &= \frac{1}{q^2} (C_{BR} + C_{SL}) g_1 + (C_{LR}^{tot} + C_{RR}) g , \\ B_2 &= \frac{1}{q^2} (C_{BR} - C_{SL}) f_1 + (C_{LR}^{tot} - C_{RR}) f , \\ G &= 4C_T g_1 , \\ N &= -4C_T \frac{1}{q^2} (f_1 + g_1) , \\ H &= N(qk) , \\ G_1 &= -8C_{TE} g_1 , \\ N_1 &= 8C_{TE} \frac{1}{q^2} (f_1 + g_1) , \\ H_1 &= N_1(qk) . \end{aligned} \quad (10)$$

In regard to the inner–Bremsstrahlung part, as a result of relevant calculations we get

$$\begin{aligned} \mathcal{M}_{IB} = & \frac{\alpha G_F}{4\sqrt{2}\pi} V_{tb} V_{tq}^* e f_B i \left\{ F \bar{\ell} \left(\frac{\not{\xi}^* \not{p}_B}{2p_1 k} - \frac{\not{p}_B \not{\xi}^*}{2p_2 k} \right) \gamma_5 \ell \right. \\ & \left. + F_1 \bar{\ell} \left[\frac{\not{\xi}^* \not{p}_B}{2p_1 k} - \frac{\not{p}_B \not{\xi}^*}{2p_2 k} + 2m_\ell \left(\frac{1}{2p_1 k} + \frac{1}{2p_2 k} \right) \not{\xi}^* \right] \ell \right\}. \end{aligned} \quad (11)$$

In deriving Eq. (11), we have used

$$\begin{aligned} \langle 0 | \bar{s} \gamma_\mu \gamma_5 b | B \rangle &= -i f_B p_{B\mu}, \\ \langle 0 | \bar{s} \sigma_{\mu\nu} (1 + \gamma_5) b | B \rangle &= 0, \end{aligned}$$

The functions F and F_1 are defined as follows

$$\begin{aligned} F &= 2m_\ell \left(C_{LR}^{tot} - C_{LL}^{tot} + C_{RL} - C_{RR} \right) + \frac{m_B^2}{m_b} \left(C_{LRLR} - C_{RLLR} - C_{LRRL} + C_{RLRL} \right), \\ F_1 &= \frac{m_B^2}{m_b} \left(C_{LRLR} - C_{RLLR} + C_{LRRL} - C_{RLRL} \right). \end{aligned} \quad (12)$$

3 Polarized forward–backward asymmetries of the leptons in $B_s \rightarrow \ell^+ \ell^- \gamma$ decay

In the present section we calculate the polarized forward–backward asymmetries of leptons. For this purpose we define the following orthogonal unit vectors s_i^\pm (here $i = L, T$ or N stands for longitudinal, transversal or normal polarizations, respectively) in the rest frame of ℓ^\pm

$$\begin{aligned} s_L^{-\mu} &= (0, \vec{e}_L^-) = \left(0, \frac{\vec{p}_-}{|\vec{p}_-|} \right), \\ s_N^{-\mu} &= (0, \vec{e}_N^-) = \left(0, \frac{\vec{p}_\Lambda \times \vec{p}_-}{|\vec{p}_\Lambda \times \vec{p}_-|} \right), \\ s_T^{-\mu} &= (0, \vec{e}_T^-) = \left(0, \vec{e}_N^- \times \vec{e}_L^- \right), \\ s_L^{+\mu} &= (0, \vec{e}_L^+) = \left(0, \frac{\vec{p}_+}{|\vec{p}_+|} \right), \\ s_N^{+\mu} &= (0, \vec{e}_N^+) = \left(0, \frac{\vec{p}_\Lambda \times \vec{p}_+}{|\vec{p}_\Lambda \times \vec{p}_+|} \right), \\ s_T^{+\mu} &= (0, \vec{e}_T^+) = \left(0, \vec{e}_N^+ \times \vec{e}_L^+ \right), \end{aligned} \quad (13)$$

where \vec{p}_\pm and \vec{k} are the three–momenta of the leptons ℓ^\pm and photon in the center of mass frame (CM) of $\ell^- \ell^+$ system, respectively. Transformation of unit vectors from the rest frame of the leptons to CM frame of leptons can be accomplished by the Lorentz boost. Boosting of the longitudinal unit vectors $s_L^{\pm\mu}$ yields

$$\left(s_L^{\mp\mu} \right)_{CM} = \left(\frac{|\vec{p}_\mp|}{m_\ell}, \frac{E_\ell \vec{p}_\mp}{m_\ell |\vec{p}_\mp|} \right), \quad (14)$$

where $\vec{p}_+ = -\vec{p}_-$, E_ℓ and m_ℓ are the energy mass of leptons in the CM frame. The remaining unit vectors $s_N^{\pm\mu}$, $s_T^{\pm\mu}$ are unchanged under Lorentz transformation.

The definition of the normalized, unpolarized differential forward-backward asymmetry is

$$\mathcal{A}_{FB} = \frac{\int_0^1 \frac{d^2\Gamma}{d\hat{s}dz} - \int_{-1}^0 \frac{d^2\Gamma}{d\hat{s}dz}}{\int_0^1 \frac{d^2\Gamma}{d\hat{s}dz} + \int_{-1}^0 \frac{d^2\Gamma}{d\hat{s}dz}}, \quad (15)$$

where $z = \cos\theta$ is the angle between Λ_b meson and ℓ^- in the center mass frame of leptons. When the spins of both leptons are taken into account, the \mathcal{A}_{FB} will be a function of the spins of the final leptons and it is defined as

$$\begin{aligned} \mathcal{A}_{FB}^{ij}(\hat{s}) &= \left(\frac{d\Gamma(\hat{s})}{d\hat{s}} \right)^{-1} \left\{ \int_0^1 dz - \int_{-1}^0 dz \right\} \left\{ \left[\frac{d^2\Gamma(\hat{s}, \vec{s}^- = \vec{i}, \vec{s}^+ = \vec{j})}{d\hat{s}dz} - \frac{d^2\Gamma(\hat{s}, \vec{s}^- = \vec{i}, \vec{s}^+ = -\vec{j})}{d\hat{s}dz} \right] \right. \\ &\quad \left. - \left[\frac{d^2\Gamma(\hat{s}, \vec{s}^- = -\vec{i}, \vec{s}^+ = \vec{j})}{d\hat{s}dz} - \frac{d^2\Gamma(\hat{s}, \vec{s}^- = -\vec{i}, \vec{s}^+ = -\vec{j})}{d\hat{s}dz} \right] \right\}, \\ &= \mathcal{A}_{FB}(\vec{s}^- = \vec{i}, \vec{s}^+ = \vec{j}) - \mathcal{A}_{FB}(\vec{s}^- = \vec{i}, \vec{s}^+ = -\vec{j}) - \mathcal{A}_{FB}(\vec{s}^- = -\vec{i}, \vec{s}^+ = \vec{j}) \\ &\quad + \mathcal{A}_{FB}(\vec{s}^- = -\vec{i}, \vec{s}^+ = -\vec{j}). \end{aligned} \quad (16)$$

Using these definitions for the double polarized FB asymmetries, we get the following results:

$$\begin{aligned} \mathcal{A}_{FB}^{LL} &= \frac{1}{\Delta} \left\{ -4m_B^2 \hat{s}(1-\hat{s})^2 v \text{Re}[A_1^* A_2 - B_1^* B_2] \right. \\ &\quad - \frac{2}{\hat{m}_\ell} m_B \hat{s}(1-\hat{s})^2 v(1-v^2) \left(\text{Im}[(A_1^* - B_1^*) G_1] - \text{Re}[(A_2 - B_2)^* G] \right) \\ &\quad - \frac{4}{\hat{m}_\ell} m_B \hat{s}^2 (1-\hat{s}) v(1-v^2) \text{Im}[(A_1^* - B_1^*) H_1] \\ &\quad + \frac{4}{\hat{m}_\ell v} f_B m_B \hat{s}(1-\hat{s})(1-v^2) \ln[1-v^2] \text{Re}[(A_2^* - B_2^*) F] \\ &\quad \left. - \frac{4}{\hat{m}_\ell v} f_B m_B \hat{s}(1-\hat{s})(1-v^2) \ln[1-v^2] \text{Re}[(A_1^* - B_1^*) F_1] \right\}, \end{aligned} \quad (17)$$

$$\begin{aligned} \mathcal{A}_{FB}^{LN} &= \frac{1}{\Delta} \left\{ -\frac{4}{3} m_B \sqrt{\hat{s}} (1-\hat{s})^2 v \text{Re}[(A_1^* - A_2^* + B_1^* + B_2^*) G_1] \right. \\ &\quad + \frac{4}{3} m_B \sqrt{\hat{s}} (1-\hat{s})^2 v \text{Im}[(A_1^* - A_2^* - B_1^* - B_2^*) G] \\ &\quad + \frac{4}{3} m_B^3 \sqrt{\hat{s}^3} (1-\hat{s})^2 v \left(\text{Re}[(A_2^* - B_2^*) N_1^*] - \text{Im}[(A_2^* + B_2^*) N] \right) \\ &\quad - \frac{2}{3\hat{m}_\ell} m_B^2 \sqrt{\hat{s}^3} (1-\hat{s})^2 v(1-v^2) \left(2\text{Re}[G^* N_1 + G_1^* N + m_B^2 \hat{s} N_1^* N] + \text{Im}[A_1^* B_1 + A_2^* B_2] \right) \\ &\quad \left. - f_B m_B^2 \sqrt{\hat{s}} (1-\hat{s}) \left\{ 2f_B m_B^2 \hat{m}_\ell \text{Im}[F_1^* F] I_4 + v [m_B (1-\hat{s}) \text{Im}[(A_1^* + B_1^*) F_1] \right. \right. \end{aligned}$$

$$\begin{aligned}
& + m_B \text{Im}[(A_1^* - A_2^* - B_1^* - B_2^*)F - \hat{s}(A_1^* + A_2^* - B_1^* + B_2^*)F] + 8\hat{m}_\ell \text{Re}[F^* H_1] I_7 \Big\} \\
& + f_B m_B^3 \sqrt{\hat{s}}(1 - \hat{s})v[1 - \hat{s}(1 - 2v^2)] \text{Im}[(A_2^* - B_2^*)F_1] \mathcal{J}_4 \\
& + 8f_B m_B^2 \hat{m}_\ell \sqrt{\hat{s}}(1 - \hat{s})v \text{Re}[F^*(G_1 + m_B^2 N_1)] \mathcal{J}_4 \\
& + 4f_B m_B^4 \hat{m}_\ell \sqrt{\hat{s}}(1 - \hat{s})^2 v \text{Im}[F_1^* N] \mathcal{J}_4 \Big\} , \tag{18}
\end{aligned}$$

$$\begin{aligned}
\mathcal{A}_{FB}^{NL} = & \frac{1}{\Delta} \Big\{ \frac{4}{3} m_B \sqrt{\hat{s}}(1 - \hat{s})^2 v \text{Re}[(A_1^* + A_2^* + B_1^* - B_2^*)G_1] \\
& + \frac{4}{3} m_B \sqrt{\hat{s}}(1 - \hat{s})^2 v \text{Im}[(A_1^* + A_2^* - B_1^* + B_2^*)G] \\
& + \frac{4}{3} m_B^3 \sqrt{\hat{s}^3}(1 - \hat{s})^2 v \left(\text{Re}[(A_2^* - B_2^*)N_1] + \text{Im}[(A_2^* + B_2^*)N] \right) \\
& + \frac{2}{3\hat{m}_\ell} m_B^2 \sqrt{\hat{s}^3}(1 - \hat{s})^2 v(1 - v^2) \left(2\text{Re}[G^* N_1 + G_1^* N + m_B^2 \hat{s} N_1^* N] - \text{Im}[A_1^* B_1 + A_2^* B_2] \right) \\
& + f_B m_B^2 \sqrt{\hat{s}}(1 - \hat{s}) \left\{ 2f_B m_B^2 \hat{m}_\ell \text{Im}[F_1^* F] I_4 + v \left[m_B(1 - \hat{s}) \text{Im}[(A_1^* + B_1^*)F_1] \right. \right. \\
& \left. \left. - m_B \text{Im}[(A_1^* + A_2^* - B_1^* + B_2^*)F - \hat{s}(A_1^* - A_2^* - B_1^* - B_2^*)F] + 8\hat{m}_\ell \text{Re}[F^* H_1] \right] I_7 \right\} \\
& + f_B m_B^3 \sqrt{\hat{s}}(1 - \hat{s})v[1 - \hat{s}(1 - 2v^2)] \text{Im}[(A_2^* - B_2^*)F_1] \mathcal{J}_4 \\
& - 8f_B m_B^2 \hat{m}_\ell \sqrt{\hat{s}}(1 - \hat{s})v \text{Re}[F^*(G_1 + m_B^2 N_1)] \mathcal{J}_4 \\
& \left. - 4f_B m_B^4 \hat{m}_\ell \sqrt{\hat{s}}(1 - \hat{s})^2 v \text{Im}[F_1^* N] \mathcal{J}_4 \right\} , \tag{19}
\end{aligned}$$

$$\begin{aligned}
\mathcal{A}_{FB}^{LT} = & \frac{1}{\Delta} \Big\{ \frac{4}{3\sqrt{\hat{s}}} \hat{m}_\ell (1 - \hat{s})^2 \left[4(|G_1|^2 + |G|^2) + m_B^2 \hat{s} (|A_1|^2 + |A_2|^2 + |B_1|^2 + |B_2|^2) \right] \\
& - \frac{4}{3} m_B \sqrt{\hat{s}}(1 - \hat{s})^2 v^2 \left(\text{Im}[(A_1^* - B_1^*)G_1] - \text{Re}[(A_2^* - B_2^*)(G + m_B^2 \hat{s} N)] \right) \\
& - \frac{4}{3} m_B \sqrt{\hat{s}}(1 - \hat{s})^2 (2 - v^2) \left(\text{Re}[(A_1^* + B_1^*)G] - \text{Im}[(A_2^* + B_2^*)(G_1 + m_B^2 \hat{s} N_1)] \right) \\
& + \frac{8}{3} m_B^2 \hat{m}_\ell \sqrt{\hat{s}}(1 - \hat{s})^2 \left(\text{Re}[A_1^* B_1 + A_2^* B_2 + 4G_1^* N_1] + 2m_B^2 \hat{s} |N_1|^2 \right) \\
& + \frac{1}{\sqrt{\hat{s}}} f_B^2 m_B^4 \hat{m}_\ell (1 - \hat{s}) \left[(1 - \hat{s}) (|F_1|^2 + |F|^2) (\mathcal{J}_1 + \mathcal{J}_2) + 2\hat{s}v |F_1|^2 \mathcal{J}_3 \right] \\
& + f_B m_B^3 \sqrt{\hat{s}}(1 - \hat{s})^2 v^2 \text{Re}[(A_1^* - B_1^*)F_1] \mathcal{J}_4 \\
& - f_B m_B^3 \sqrt{\hat{s}}(1 - \hat{s})^2 v^2 \text{Re}[(A_2^* - B_2^*)F^*] \mathcal{J}_4 \\
& + f_B m_B^3 \sqrt{\hat{s}}(1 - \hat{s})^2 (2 - v^2) \text{Re}[(A_1^* + B_1^*)F] \mathcal{J}_4 \\
& - 4f_B m_B^4 \hat{m}_\ell \sqrt{\hat{s}}(1 - \hat{s}) [2 + v^2 - \hat{s}(2 - v^2)] \text{Im}[F_1^* N_1] \mathcal{J}_4 \\
& + 8f_B m_B^2 \hat{m}_\ell \sqrt{\hat{s}}(1 - \hat{s}) v^2 \text{Im}[F_1^* H_1] \mathcal{J}_4 \\
& - f_B m_B^3 \sqrt{\hat{s}}(1 - \hat{s}) [2 - v^2 - \hat{s}(2 - 3v^2)] \text{Re}[(A_2^* + B_2^*)F_1] \mathcal{J}_4 \\
& \left. - \frac{8}{\sqrt{\hat{s}}} f_B m_B^2 \hat{m}_\ell (1 - \hat{s}) \left[(1 - \hat{s} + \hat{s}v^2) \text{Im}[F_1^* G_1] + (1 - \hat{s}) \text{Re}[F^* G] \right] \mathcal{J}_4 \right\} , \tag{20}
\end{aligned}$$

$$\begin{aligned}
\mathcal{A}_{FB}^{TL} = \frac{1}{\Delta} \left\{ & -\frac{4}{3\sqrt{\hat{s}}}\hat{m}_\ell(1-\hat{s})^2 \left[4(|G_1|^2 + |G|^2) + m_B^2\hat{s}(|A_1|^2 + |A_2|^2 + |B_1|^2 + |B_2|^2) \right] \right. \\
& - \frac{4}{3}m_B\sqrt{\hat{s}}(1-\hat{s})^2v^2 \left(\text{Im}[(A_1^* - B_1^*)G_1] - \text{Re}[(A_2^* - B_2^*)(G + m_B^2\hat{s}N)] \right) \\
& + \frac{4}{3}m_B\sqrt{\hat{s}}(1-\hat{s})^2(2-v^2) \left(\text{Re}[(A_1^* + B_1^*)G] - \text{Im}[(A_2^* + B_2^*)(G_1 + m_B^2\hat{s}N_1)] \right) \\
& - \frac{8}{3}m_B^2\hat{m}_\ell\sqrt{\hat{s}}(1-\hat{s})^2 \left(\text{Re}[A_1^*B_1 + A_2^*B_2 + 4G_1^*N_1] + 2m_B^2\hat{s}|N_1|^2 \right) \\
& - \frac{1}{\sqrt{\hat{s}}}f_B^2m_B^4\hat{m}_\ell(1-\hat{s}) \left[(1-\hat{s}) \left(|F_1|^2 + |F|^2 \right) (\mathcal{J}_1 + \mathcal{J}_2) + 2\hat{s}v|F_1|^2\mathcal{J}_3 \right] \\
& + f_Bm_B^3\sqrt{\hat{s}}(1-\hat{s})^2v^2\text{Re}[(A_1^* - B_1^*)F_1]\mathcal{J}_4 \\
& - f_Bm_B^3\sqrt{\hat{s}}(1-\hat{s})^2v^2\text{Re}[(A_2^* - B_2^*)F]\mathcal{J}_4 \\
& - f_Bm_B^3\sqrt{\hat{s}}(1-\hat{s})^2(2-v^2)\text{Re}[(A_1^* + B_1^*)F]\mathcal{J}_4 \\
& + 4f_Bm_B^4\hat{m}_\ell\sqrt{\hat{s}}(1-\hat{s})[2+v^2-\hat{s}(2-v^2)]\text{Im}[F_1^*N_1]\mathcal{J}_4 \\
& - 8f_Bm_B^2\hat{m}_\ell\sqrt{\hat{s}}(1-\hat{s})v^2\text{Im}[F_1^*H_1]\mathcal{J}_4 \\
& + f_Bm_B^3\sqrt{\hat{s}}(1-\hat{s})[2-v^2-\hat{s}(2-3v^2)]\text{Re}[(A_2^* + B_2^*)F_1]\mathcal{J}_4 \\
& \left. + \frac{8}{\sqrt{\hat{s}}}f_Bm_B^2\hat{m}_\ell(1-\hat{s}) \left[(1-\hat{s} + \hat{s}v^2)\text{Im}[F_1^*G_1] + (1-\hat{s})\text{Re}[F^*G] \right] \mathcal{J}_4 \right\}, \tag{21}
\end{aligned}$$

where,

$$\begin{aligned}
\Delta = & 16m_B\hat{m}_\ell(1-\hat{s})^2 \left(\text{Im}[(A_2^* + B_2^*)G_1] - \text{Re}[(A_1^* + B_1^*)G - m_B\hat{m}_\ell(A_1^*B_1 + A_2^*B_2)] \right) \\
& + 48m_B\hat{m}_\ell\hat{s}(1-\hat{s})\text{Im}[(A_2^* + B_2^*)H_1] \\
& - 8m_B^3\hat{m}_\ell\hat{s}(1-\hat{s})^2\text{Im}[(A_2^* + B_2^*)N_1] \\
& + \frac{2}{3}(1-\hat{s})^2 \left[4(3-v^2)(|G_1|^2 + |G|^2) + m_B^2\hat{s}(3+v^2)(|A_1|^2 + |A_2|^2 + |B_1|^2 + |B_2|^2) \right] \\
& + 16\hat{s}v^2 \left[(1-\hat{s})\text{Re}[G^*H] + \hat{s}|H|^2 \right] \\
& + 16\hat{s}(3-2v^2) \left[(1-\hat{s})\text{Re}[G_1^*H_1] + \hat{s}|H_1|^2 \right] \\
& - \frac{4}{3}m_B^2\hat{s}(1-\hat{s})^2(3-2v^2) \left(2\text{Re}[G_1^*N_1] + m_B^2\hat{s}|N_1|^2 \right) \\
& - \frac{4}{3}m_B^2\hat{s}(1-\hat{s})^2v^2 \left(2\text{Re}[G^*N] + m_B^2\hat{s}|N|^2 \right) \\
& - \frac{1}{2}f_B^2m_B^4|F|^2 \left\{ (1-\hat{s})^2v^2(\mathcal{I}_1 + \mathcal{I}_3) - (1+\hat{s}^2 + 2\hat{s}v^2)\mathcal{I}_2 - [1-\hat{s}(4-\hat{s}-2v^2)]\mathcal{I}_5 \right\} \\
& + \frac{1}{2}f_B^2m_B^4|F_1|^2 \left\{ -(1-\hat{s})^2v^2(\mathcal{I}_1 + \mathcal{I}_3) + [1-\hat{s}(2-\hat{s}-4v^2 + 2\hat{s}v^2 - 2\hat{s}v^4)]\mathcal{I}_2 \right. \\
& \left. - 2\hat{s}(1-\hat{s})v(1-v^2)\mathcal{I}_4 + [1-\hat{s}(2-\hat{s} + 2\hat{s}v^2 - 2\hat{s}v^4)]\mathcal{I}_5 \right\} \\
& - 4f_Bm_B^2\hat{s}v\text{Re}[F^*H] \left[(1-\hat{s})v\mathcal{I}_6 + (1+\hat{s})\mathcal{I}_7 \right] \\
& - 4f_Bm_B^2\hat{s}\text{Im}[F_1^*H_1] \left[(1-\hat{s})v^2\mathcal{I}_6 + (3-2v^2-3\hat{s} + 4\hat{s}v^2)\mathcal{I}_7 \right] \\
& + 2f_Bm_B\hat{m}_\ell\text{Re}[(A_1^* + B_1^*)F] \left[8(1+\hat{s}) + m_B^2(1-\hat{s}^2)v^2\mathcal{I}_6 + m_B^2(1-\hat{s})(1-3\hat{s})\mathcal{I}_7 \right]
\end{aligned}$$

$$\begin{aligned}
& - f_B m_B \hat{m}_\ell (1 - \hat{s}) \text{Re}[(A_2^* + B_2^*) F_1] \left[8 + m_B^2 (1 - 5\hat{s}) v^2 \mathcal{I}_6 + m_B^2 (3 - 3\hat{s} + 4\hat{s}v^2) \mathcal{I}_7 \right] \\
& + f_B \text{Im}[F_1^* G_1] \left[-24(1 - \hat{s} + 2\hat{s}v^2) + m_B^2 (1 - \hat{s})(1 + 3\hat{s} - 6\hat{s}v^2) v^2 \mathcal{I}_6 \right. \\
& \left. - m_B^2 (1 - \hat{s})(1 - \hat{s} - 2\hat{s}v^2) \mathcal{I}_7 \right] \\
& + f_B \text{Re}[F^* G] \left[-24(1 + \hat{s}) + m_B^2 (1 - \hat{s})(1 - 3\hat{s}) v^2 \mathcal{I}_6 - m_B^2 (1 - \hat{s})(1 - 7\hat{s} + 4\hat{s}v^2) \mathcal{I}_7 \right] \\
& + f_B m_B^2 \hat{s} \text{Im}[F_1^* N_1] \left[-8(1 - \hat{s} + 2\hat{s}v^2) + m_B^2 (1 - \hat{s})(3 + \hat{s} - 2\hat{s}v^2) v^2 \mathcal{I}_6 \right. \\
& \left. + m_B^2 (1 - \hat{s})(3 - 2v^2 - 3\hat{s} + 4\hat{s}v^2) \mathcal{I}_7 \right] \\
& + f_B m_B^2 \hat{s} \text{Re}[F^* N] \left[-8(1 + \hat{s}) + m_B^2 (1 - \hat{s})(3 - \hat{s}) v^2 \mathcal{I}_6 + m_B^2 (1 - \hat{s}^2) \mathcal{I}_7 \right] . \tag{22}
\end{aligned}$$

In Eqs. (16)–(22), $\hat{s} = q^2/m_B^2$, $v = \sqrt{1 - 4\hat{m}_\ell^2/\hat{s}}$ is the lepton velocity with $\hat{m}_\ell = m_\ell/m_B$, and \mathcal{I}_i represent the following integrals

$$\begin{aligned}
\mathcal{I}_i &= \int_{-1}^{+1} \mathcal{F}_i(z) dz , \\
\mathcal{J}_i &= \int_0^{+1} \mathcal{G}_i(z) dz - \int_{-1}^0 \mathcal{G}_i(z) dz ,
\end{aligned}$$

where

$$\begin{aligned}
\mathcal{G}_1 &= \frac{z\sqrt{1-z^2}}{(p_1 \cdot k)(p_2 \cdot k)} , & \mathcal{G}_2 &= \frac{z\sqrt{1-z^2}}{(p_1 \cdot k)^2} , & \mathcal{G}_3 &= \frac{\sqrt{1-z^2}}{(p_1 \cdot k)^2} , \\
\mathcal{G}_4 &= \frac{z\sqrt{1-z^2}}{(p_1 \cdot k)} , & \mathcal{F}_1 &= \frac{z^2}{(p_1 \cdot k)(p_2 \cdot k)} , & \mathcal{F}_2 &= \frac{1}{(p_1 \cdot k)(p_2 \cdot k)} , \\
\mathcal{F}_3 &= \frac{z^2}{(p_1 \cdot k)^2} , & \mathcal{F}_4 &= \frac{z}{(p_1 \cdot k)^2} , & \mathcal{F}_5 &= \frac{1}{(p_1 \cdot k)^2} , \\
\mathcal{F}_6 &= \frac{z^2}{p_1 \cdot k} , & \mathcal{F}_7 &= \frac{1}{p_1 \cdot k} .
\end{aligned}$$

We note that, the forward–backward asymmetries \mathcal{A}_{NN} , \mathcal{A}_{NT} , \mathcal{A}_{TN} and \mathcal{A}_{TT} are all equal to zero.

4 Numerical analysis and discussion

In this section we present our numerical analysis for all possible polarized forward–backward asymmetries of leptons. The values of the input parameters which we have used in the numerical analysis are: $|V_{tb}V_{ts}^*| = 0.0385$, $m_\mu = 0.106 \text{ GeV}$, $m_\tau = 1.78 \text{ GeV}$, $m_b = 4.8 \text{ GeV}$. For the SM values of the Wilson coefficients we have used $C_7^{SM}(m_b) = -0.313$, $C_9^{SM}(m_b) = 4.344$ and $C_{10}^{SM}(m_b) = -4.669$. The magnitude of C_7^{SM} is quite well determined from the $b \rightarrow s\gamma$ transition, and hence it is well established. Therefore the values of C_{BR} and C_{SL} are fixed by the relations $C_{BR} = -2m_b C_7^{eff}$ and $C_{SL} = -2m_s C_7^{eff}$. It is well known that the Wilson coefficient C_9^{SM} receives also long distance contributions which have their origin

in the real $\bar{c}c$ intermediate states, i.e., $J/\psi, \psi', \dots$ [15]. In the present work we consider only short distance contributions.

The values of the new Wilson coefficients are needed in order to carry out the numerical calculations for \mathcal{A}_{ij} given in Eqs. (17)–(22). All new Wilson coefficients are varied in the range $-|C_{10}^{SM}| \leq C_X \leq |C_{10}^{SM}|$ and it is assumed that they are real. The experimental results on the branching ratio of the $B_s \rightarrow K^*(K)\ell^+\ell^-$ decays [16, 17] and the bound on the branching ratio of $B_s \rightarrow \mu^+\mu^-$ [18] suggest that this is the right order of magnitude for the Wilson coefficients describing the vector and scalar interaction coefficients. But present experimental results on the branching ratio of the $B_s \rightarrow K^*\ell^+\ell^-$ and $B_s \rightarrow K\ell^+\ell^-$ decays impose stronger restrictions on some of the new Wilson coefficients. For example, $-2 \leq C_{LL} \leq 0$, $0 \leq C_{RL} \leq 2.3$, $-1.5 \leq C_T \leq 1.5$ and $-3.3 \leq C_{TE} \leq 2.6$, and all of the remaining Wilson coefficients vary in the region $-|C_{10}^{SM}| \leq C_X \leq |C_{10}^{SM}|$.

It follows from the expressions of all forward–backward asymmetries of the leptons that, explicit forms of the form factors are needed, which are the main and most important parameters in the calculation of \mathcal{A}_{ij} . These form factors are calculated in the framework of the QCD sum rules in [3, 13, 14] whose q^2 dependences are given as

$$g(q^2) = \frac{1 \text{ GeV}}{\left(1 - \frac{q^2}{(5.6 \text{ GeV})^2}\right)^2}, \quad f(q^2) = \frac{0.8 \text{ GeV}}{\left(1 - \frac{q^2}{(6.5 \text{ GeV})^2}\right)^2},$$

$$g_1(q^2) = \frac{3.74 \text{ GeV}^2}{\left(1 - \frac{q^2}{40.5 \text{ GeV}^2}\right)^2}, \quad f_1(q^2) = \frac{0.67 \text{ GeV}^2}{\left(1 - \frac{q^2}{30 \text{ GeV}^2}\right)^2},$$

which we will use in the numerical analysis.

Numerical results are presented only for the $B_s \rightarrow \ell^+\ell^-\gamma$ decay, because in the SU(3) limit the difference between the decay rates of $B_s \rightarrow \ell^+\ell^-\gamma$ and $B_d \rightarrow \ell^+\ell^-\gamma$ is attributed only to the CKM matrix elements. In other words, the decay rate of the $B_s \rightarrow \ell^+\ell^-\gamma$ is approximately 20 times larger compared to that of decay rate of $B_d \rightarrow \ell^+\ell^-\gamma$, that is

$$\frac{\Gamma(B_d \rightarrow \ell^+\ell^-\gamma)}{\Gamma(B_s \rightarrow \ell^+\ell^-\gamma)} \simeq \frac{|V_{tb}V_{td}^*|^2}{|V_{tb}V_{ts}^*|^2} \simeq \frac{1}{20}.$$

We now proceed by commenting on the result of our numerical analysis. Firstly, we study the dependence of the polarized forward–backward asymmetries on q^2 at five different values of the new Wilson coefficients. Our detailed numerical analysis shows that for the $B_s \rightarrow \mu^+\mu^-\gamma$ decay only the \mathcal{A}_{FB}^{LT} and \mathcal{A}_{FB}^{TL} asymmetries have zero positions (the numerical values of the asymmetries \mathcal{A}_{FB}^{LN} and \mathcal{A}_{FB}^{NL} are very small and hence we do not present them). In Fig. (1) we present the dependence of \mathcal{A}_{FB}^{LT} on q^2 at five fixed values of the scalar interaction coefficient $C_{LRLR} = -4; -2; 0; +2; +4$. From this figure we see that the zero position which occurs for positive values of C_{LRLR} is shifted to right for increasing values of C_{LRLR} . The same figure also depicts that the zero position of \mathcal{A}_{FB}^{LT} is absent for the SM case. Therefore, determination of the zero position of \mathcal{A}_{FB}^{LT} is an unambiguous indication of the new physics beyond the SM, as well as allowing us determine the sign of the scalar

interaction coefficients C_{LRLR} . In Fig. (2) we present the dependence of \mathcal{A}_{FB}^{LT} on q^2 at fixed values of C_{RLLR} . Similar to the previous case, zero position of the \mathcal{A}_{FB}^{LT} appears again, but the difference from it being it occurs for the negative values of C_{RLLR} . It should be noted here that the zero position of \mathcal{A}_{FB}^{LT} is present for the remaining scalar interaction coefficients C_{LRRL} and C_{RLRL} as well, which can be seen in Figs. (3) and (4). More interesting observation for these cases is that, the zero position appears for $q^2 < 2 \text{ GeV}^2$ and hence it is free of the long distance J/ψ contributions. As far as $B_s \rightarrow \mu^+ \mu^- \gamma$ decay is concerned, our numerical analysis shows that the zero position of \mathcal{A}_{FB}^{LT} is absent for all Wilson coefficients other than the scalar interaction coefficients. Hence, determination of the zero position of \mathcal{A}_{FB}^{LT} can serve as a good test for establishing new physics beyond the SM due to the presence of the scalar interaction coefficients.

The situation for the \mathcal{A}_{FB}^{TL} asymmetry for the $B_s \rightarrow \mu^+ \mu^- \gamma$ decay is richer in content compared to that of the \mathcal{A}_{FB}^{LT} case. For this forward–backward asymmetry, the zero position occurs for all new Wilson coefficients. In Figs. (5)–(11) we present the dependence of \mathcal{A}_{FB}^{TL} on q^2 at five fixed values of the new Wilson coefficients. These figures depict that:

- For vector interactions with the Wilson coefficients C_{LL} and C_{RR} , the zero position of \mathcal{A}_{FB}^{TL} is shifted. When these coefficients get positive (negative) values, the zero position of \mathcal{A}_{FB}^{TL} is shifted to the left (right) compared to that of the SM case. In the presence of the Wilson coefficients C_{LR} and C_{RL} the zero position of the \mathcal{A}_{FB}^{TL} is shifted to the right (left) compared to that of the SM result, when these Wilson coefficients are positive (negative).
- In the presence of the scalar interactions with the coefficients C_{LRRL} and C_{RLRL} , the zero position of \mathcal{A}_{FB}^{TL} is shifted the left compared to that of the SM result. The zero position for C_{LRRL} occurs only for its positive values, while it occurs only for the negative values of C_{RLRL} .

In the presence of scalar interactions C_{RLLR} and C_{LRLR} , no new zero position of \mathcal{A}_{FB}^{TL} occurs with respect to the one for the SM case.

- New zero positions of \mathcal{A}_{FB}^{TL} are observed in the presence of the tensor interaction for the positive values of C_T , and the zero position is shifted to the left,

In the case of $B_s \rightarrow \tau^+ \tau^- \gamma$ decay, similar to the $B_s \rightarrow \mu^+ \mu^- \gamma$ decay, we observe that several of the polarized forward–backward asymmetries are very sensitive to the existence of new physics. Let us briefly summarize our results:

i) Among all polarization asymmetries (which can be measurable in the experiments) only \mathcal{A}_{FB}^{TL} is very sensitive to the existence of all types of new physics interactions, except to the presence of the vector interactions with coefficients C_{LL} and C_{RR} .

ii) \mathcal{A}_{FB}^{LL} is sensitive to the presence of the tensor interaction and its zero position occurs for $C_T = +4$ at $q^2 \approx 17 \text{ GeV}^2$, while zero position of \mathcal{A}_{FB}^{LL} is absent for the SM case. Therefore, determination of the zero position of \mathcal{A}_{FB}^{LL} can confirm the existence of the tensor interaction in the $B_s \rightarrow \tau^+ \tau^- \gamma$ decay (see Fig. (12)).

- \mathcal{A}_{FB}^{TL} exhibits similar dependence on C_{LR} and C_{RL} . The zero position of \mathcal{A}_{FB}^{TL} is shifted to to the left (right) when C_{LR} and C_{RL} are negative (positive) compared to that of

the SM prediction. Note that the zero position of \mathcal{A}_{FB}^{TL} lies on the left side for the vector interaction C_{LR} compared to the zero position of the C_{RL} (see Figs. (13), (14)).

- \mathcal{A}_{FB}^{TL} shows stronger dependence on the scalar interactions C_{LRRL} and C_{RLRL} . The magnitude of \mathcal{A}_{FB}^{TL} increases (decreases) as the new Wilson coefficient C_{LRRL} gets positive (negative) values. This behavior is to the contrary for the coefficient C_{RLRL} (see Figs. (15), (16)).
- In the presence of the tensor interaction with the coefficient C_T , zero position of the asymmetry \mathcal{A}_{FB}^{TL} is located on the left side of the SM prediction for negative values of C_T (Fig. (17)).

We see from the explicit expressions of the polarized forward–backward asymmetries that they all depend both on q^2 and the new Wilson coefficients. For this reason there may appear difficulties in the experiments in studying the dependence of the physical observables on both parameters simultaneously. In order to get "pure information" about about new physics, we eliminate the dependence of physical quantities on q^{\oplus} , by performing integration over q^2 in the kinematically allowed region, i.e., we average the polarized forward backward asymmetry

$$\langle \mathcal{A}_{ij} \rangle = \frac{\int_{4m_\ell^2}^{m_B^2} \mathcal{A}_{ij} \frac{d\mathcal{B}}{dq^2} dq^2}{\int_{4m_\ell^2}^{m_B^2} \frac{d\mathcal{B}}{dq^2} dq^2} .$$

In Fig. (18) we depict the dependence of $\langle \mathcal{A}_{FB}^{LL} \rangle$ on the new Wilson for the $B_s \rightarrow \mu^+ \mu^- \gamma$ decay. From this figure we see that $\langle \mathcal{A}_{FB}^{LL} \rangle$ shows symmetric behavior in its dependence on all scalar interactions; and except for regions $-4 < C_{RR}, C_{RL} < 0$, $-0.4 < C_{LRRL}, C_{LRRR} < 0$ and $0 \leq C_{RLRL}, C_{LRLR} < 0.4$ it is larger compared to the SM result (SM result corresponds to the intersection point of all curves). It is also interesting to observe that $\langle \mathcal{A}_{FB}^{LL} \rangle > \langle \mathcal{A}_{FB}^{SM} \rangle$ for only negative values of C_{RR} .

Our numerical analysis furthers shows that, for the $B_s \rightarrow \mu^+ \mu^- \gamma$ decay, $\langle \mathcal{A}_{FB}^{LT} \rangle$ is sensitive only to C_T and at negative (positive) values of C_T $\langle \mathcal{A}_{FB}^{LT} \rangle$ is positive (negative) and larger (smaller) compared to the SM result. Therefore, determination of the sign and magnitude of $\langle \mathcal{A}_{FB}^{LT} \rangle$ can serve as a good test for establishing existence of the tensor interaction.

The dependence of $\langle \mathcal{A}_{FB}^{TL} \rangle$ on the new Wilson coefficients for the $B_s \rightarrow \mu^+ \mu^- \gamma$ decay is presented in Fig. (19). We observe from this figure that $\langle \mathcal{A}_{FB}^{TL} \rangle$ shows stronger dependence on the tensor interaction coefficient C_T and scalar interactions C_{RLRLR} and C_{LRRR} .

In Figs. (20), (21), and (22) we present the dependence of $\langle \mathcal{A}_{FB}^{LL} \rangle$, $\langle \mathcal{A}_{FB}^{LT} \rangle$ and $\langle \mathcal{A}_{FB}^{TL} \rangle$ on the new Wilson coefficients for the $B_s \rightarrow \tau^+ \tau^- \gamma$ decay, respectively. Fig. (20) depicts that $\langle \mathcal{A}_{FB}^{LL} \rangle$ exhibits considerable departure from the SM result for the scalar interactions and the vector interaction with coefficient C_{RR} . We see from Fig. (21) that when new Wilson coefficients are negative $\langle \mathcal{A}_{FB}^{LT} \rangle$ shows stronger dependence on on the tensor interaction

(C_T) and scalar type interactions, and when $C_X > 0$, $\langle \mathcal{A}_{FB}^{LT} \rangle$ exhibits strong dependence on vector interactions and the tensor interaction with the coefficient C_{TE} .

At the end of this section, we discuss the problem of the detectability of forward–backward asymmetry in the experiments. Experimentally, to measure an asymmetry $\langle \mathcal{A}_{ij} \rangle$ of the decay with the branching ratio \mathcal{B} at $n\sigma$ level, the required number of events (i.e., the number of $B\bar{B}$ pair) are given by

$$\mathcal{N} = \frac{n^2}{\mathcal{B}s_1s_2\langle \mathcal{A}_{ij} \rangle^2},$$

where s_1 and s_2 are the efficiencies of the leptons. Efficiency of the μ lepton is practically equal to one, and typical values of the efficiency of the τ lepton ranges from 50% to 90% for the various decay modes [19].

From the expression for \mathcal{N} we see that, in order to obtain the forward–backward asymmetries in $B_s \rightarrow \ell^+\ell^-\gamma$ decays at 3σ level, the minimum number of required events are (for the efficiency of τ -lepton we take 0.5, and for $\langle \mathcal{A}_{ij} \rangle$, their maximal values beyond the SM):

- for the $B_s \rightarrow \mu^+\mu^-\gamma$ decay

$$\mathcal{N} = \begin{cases} \sim 2 \times 10^9 & \langle \mathcal{A}_{LL} \rangle, \\ \sim 3 \times 10^{10} & \langle \mathcal{A}_{LT} \rangle \simeq \langle \mathcal{A}_{TL} \rangle, \end{cases}$$

which yields that, for detecting $\langle \mathcal{A}_{LT} \rangle$ and $\langle \mathcal{A}_{TL} \rangle$, more than 10^{13} $\bar{B}B$ pairs are required.

- for $B_s \rightarrow \tau^+\tau^-\gamma$ decay

$$\mathcal{N} \simeq 6 \times 10^{11} \langle \mathcal{A}_{LL} \rangle, \langle \mathcal{A}_{LT} \rangle, \langle \mathcal{A}_{TL} \rangle.$$

The number of $\bar{B}B$ pairs that will be produced at LHC is around $\sim 10^{12}$. As a result of a comparison of this number of $\bar{B}B$ pairs with that of \mathcal{N} , we conclude that $\langle \mathcal{A}_{LL} \rangle$, $\langle \mathcal{A}_{TL} \rangle$ and $\langle \mathcal{A}_{LT} \rangle$ in both decays can be detectable in "beyond the SM scenarios" in future experiments at LHC. Note that in the SM, only $\langle \mathcal{A}_{LL} \rangle$ for the $B_s \rightarrow \mu^+\mu^-\gamma$ decay can be detectable at LHC. Therefore, observation of these asymmetries can be explained only by new physics beyond the SM.

In conclusion, we calculate polarized forward–backward asymmetries using the most general, model independent form of the effective Hamiltonian including all possible form of interactions. The sensitivity of the averaged polarized forward–backward asymmetries to the new Wilson coefficients are studied. Finally we discuss the possibility of experimental measurement of these double–lepton polarization asymmetries at LHC.

References

- [1] M. Battaglia *et al.*, prep: hep-ph/0304132 (2003).
- [2] P. Ball *et al.*, B Decays, in Proceedings of the workshop on Standard Model Physics (and more) at the LHC, CERN 2000-004 (2000).
- [3] T. M. Aliev, A. Özpineci and M. Savcı, *Phys. Rev. D* **55**, 7059 (1997).
- [4] C. Q. Geng, C. C. Lih and Wei-Min Zhang, *Phys. Rev. D* **62**, 074017 (2000).
- [5] Y. Dincer and L. M. Sehgal, *Phys. Lett. B* **521**, 7 (2000).
- [6] S. Descotes-Genon, C. T. Sachrajda, *Phys. Lett. B* **557**, 213 (2003).
- [7] F. Krüger and D. Melikhov, *Phys. Rev. D* **67**, 034002 (2003).
- [8] T. M. Aliev, A. Özpineci and M. Savcı, *Phys. Lett. B* **520**, 69 (2001); T. M. Aliev, A. Özpineci and M. Savcı, *Eur. J. Phys. C* **27**, 405 (2003); G. Eilam, C. D. Lu, D. X. Zhang *Phys. Lett. B* **391**, 461 (1997).
- [9] D. Melikhov and N. Nikitin, prep: hep-ph/0410146 (2004).
- [10] W. Bensalem, D. London, N. Sinha and R. Sinha, *Phys. Rev. D* **67**, 034007 (2003).
- [11] T. M. Aliev, V. Bashiry and M. Savcı, prep: hep-ph/0411327 (2004).
- [12] S. Fukae, C. S. Kim, T. Morozumi and T. Yoshikawa, *Phys. Rev. D* **59**, 074013 (1999).
- [13] G. Eilam, I. Halperin and R. R. Mendel *Phys. Lett. B* **361**, 137 (1995).
- [14] T. M. Aliev, N. K. Pak and M. Savcı, *Phys. Lett. B* **424**, 175 (1998).
- [15] C. S. Lim, T. Morozumi and A. I. Sanda, *Phys. Lett. B* **218**, 343 (1989); N. G. Deshpande, J. Trampetic and K. Panose, *Phys. Rev. D* **39**, 1461 (1989); A. I. Vainshtein, V. I. Zakharov, L. B. Okun and M. A. Shifman, *Sov. J. Nucl. Phys.* **24**, 427 (1976).
- [16] A. Ishikawa *et. al.*, BELLE Collaboration, *Phys. Rev. Lett.* **91**, 261601 (2003).
- [17] B. Aubert *et. al.*, BaBar Collaboration, *Phys. Rev. Lett.* **91**, 221802 (2003).
- [18] M. C. Chang *et al.*, BELLE Collaboration, *Phys. Rev. D* **67**, 111101 (2003).
- [19] G. Abbiendi *et. al.*, OPAL Collaboration, *Phys. Lett. B* **492**, 23 (2000).

Figure captions

Fig. (1) The dependence of the polarized forward–backward asymmetry \mathcal{A}_{FB}^{LT} on q^2 at four fixed values of C_{LRRL} for the $B_s \rightarrow \mu^+ \mu^- \gamma$ decay.

Fig. (2) The same as in Fig. (1), but for at four fixed values of C_{RLLR} .

Fig. (3) The same as in Fig. (1), but for at four fixed values of C_{LRRL} .

Fig. (4) The same as in Fig. (1), but for at four fixed values of C_{RLRL} .

Fig. (5) The dependence of the polarized forward–backward asymmetry \mathcal{A}_{FB}^{TL} on q^2 at four fixed values of C_{LL} for the $B_s \rightarrow \mu^+ \mu^- \gamma$ decay.

Fig. (6) The same as in Fig. (5), but for at four fixed values of C_{LR} .

Fig. (7) The same as in Fig. (5), but for at four fixed values of C_{RL} .

Fig. (8) The same as in Fig. (5), but for at four fixed values of C_{RR} .

Fig. (9) The same as in Fig. (5), but for at four fixed values of C_{LRRL} .

Fig. (10) The same as in Fig. (5), but for at four fixed values of C_{RLRL} .

Fig. (11) The same as in Fig. (5), but for at four fixed values of C_T .

Fig. (12) The dependence of the polarized forward–backward asymmetry \mathcal{A}_{FB}^{LL} on q^2 at four fixed values of C_T for the $B_s \rightarrow \tau^+ \tau^- \gamma$ decay.

Fig. (13) The dependence of the polarized forward–backward asymmetry \mathcal{A}_{FB}^{TL} on q^2 at four fixed values of C_{LR} for the $B_s \rightarrow \tau^+ \tau^- \gamma$ decay.

Fig. (14) The same as in Fig. (13), but for at four fixed values of C_{RL} .

Fig. (15) The same as in Fig. (13), but for at four fixed values of C_{LRRL} .

Fig. (16) The same as in Fig. (13), but for at four fixed values of C_{RLRL} .

Fig. (17) The same as in Fig. (13), but for at four fixed values of C_T .

Fig. (18) The dependence of the polarized forward–backward asymmetry \mathcal{A}_{FB}^{LL} on the new Wilson coefficients for the $B_s \rightarrow \mu^+ \mu^- \gamma$ decay.

Fig. (19) The same as in Fig. (18), but for the polarized forward–backward asymmetry \mathcal{A}_{FB}^{TL} .

Fig. (20) The same as in Fig. (18), but for the $B_s \rightarrow \tau^+ \tau^- \gamma$ decay.

Fig. (21) The same as in Fig. (20), but for the polarized forward–backward asymmetry \mathcal{A}_{FB}^{LT} .

Fig. (22) The same as in Fig. (21), but for the polarized forward–backward asymmetry \mathcal{A}_{FB}^{TL} .

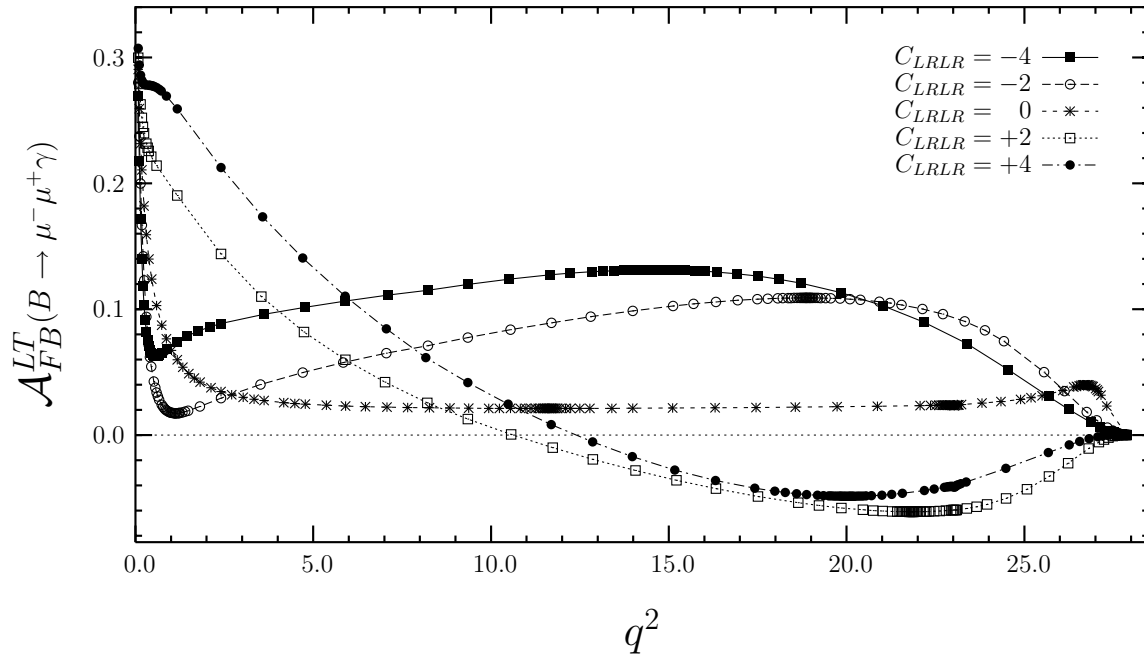


Figure 1:

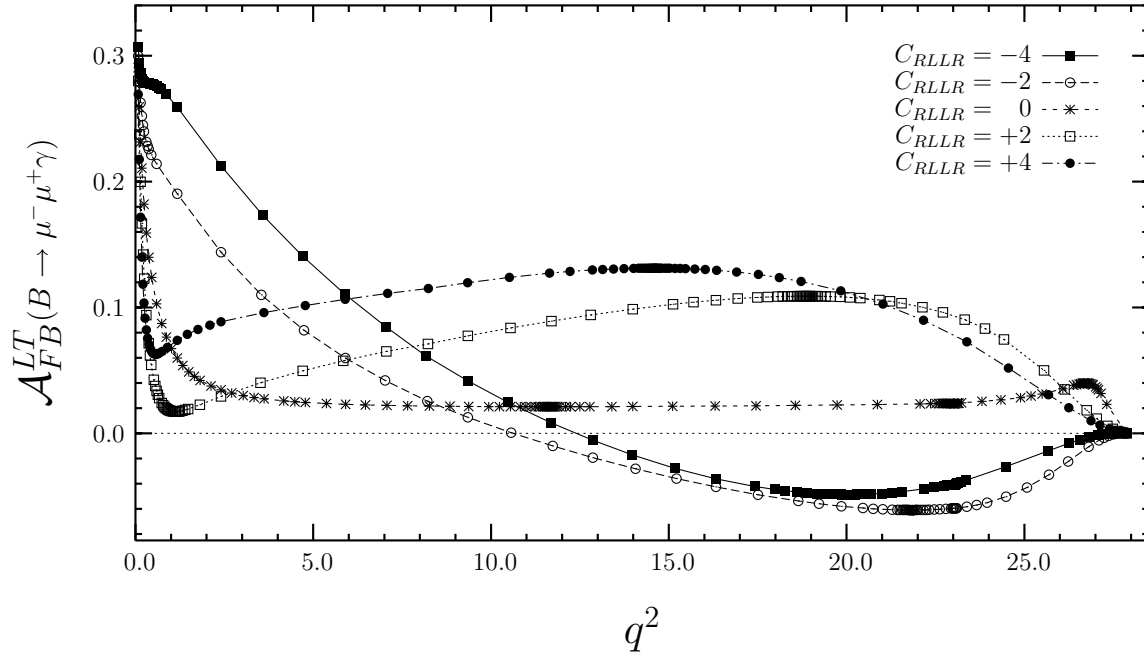


Figure 2:

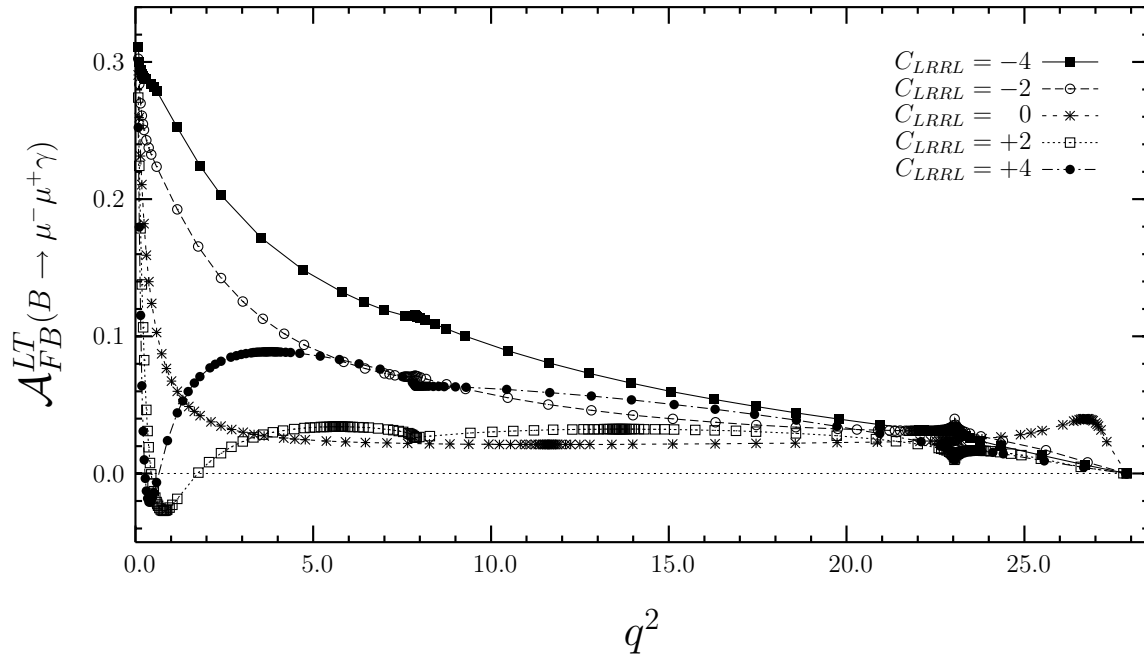


Figure 3:

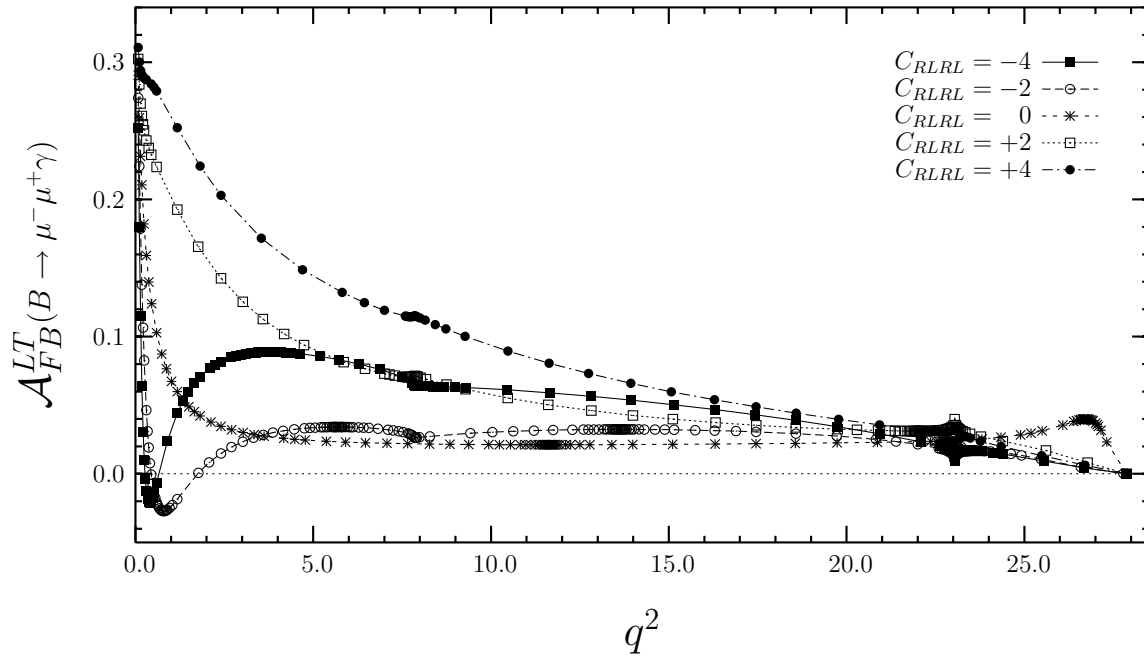


Figure 4:

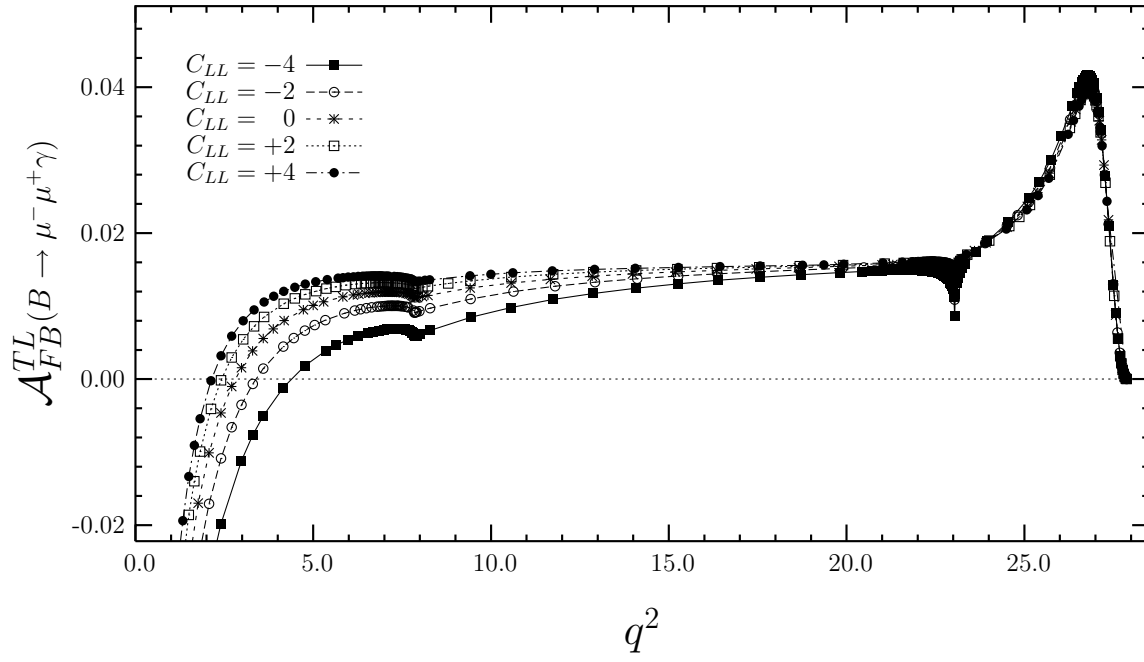


Figure 5:

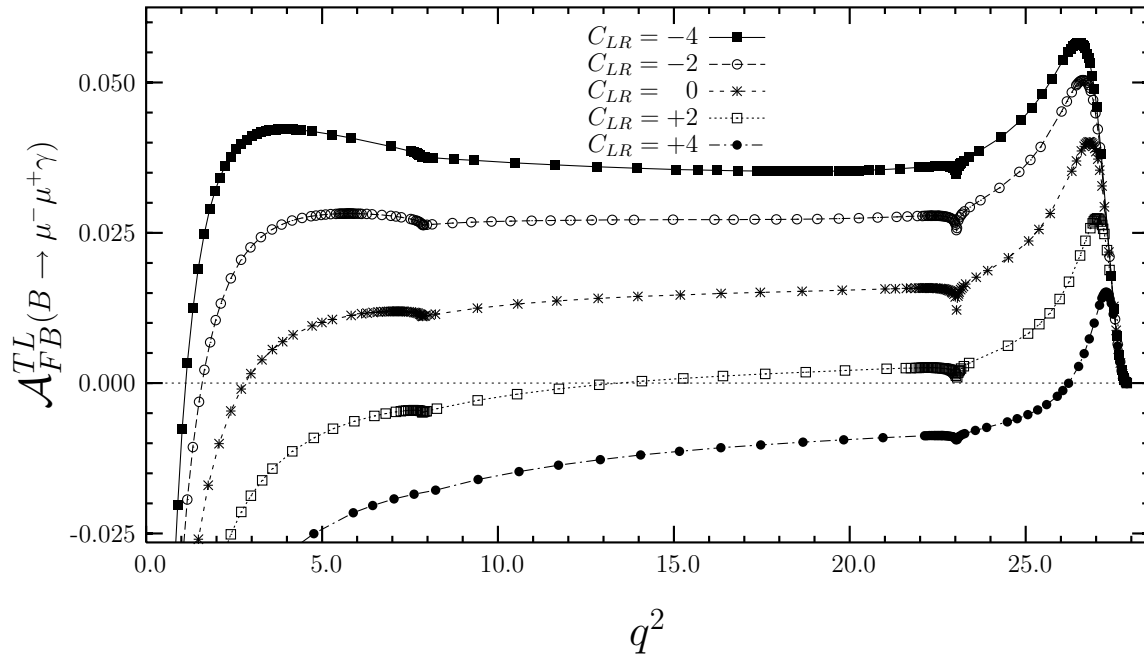


Figure 6:

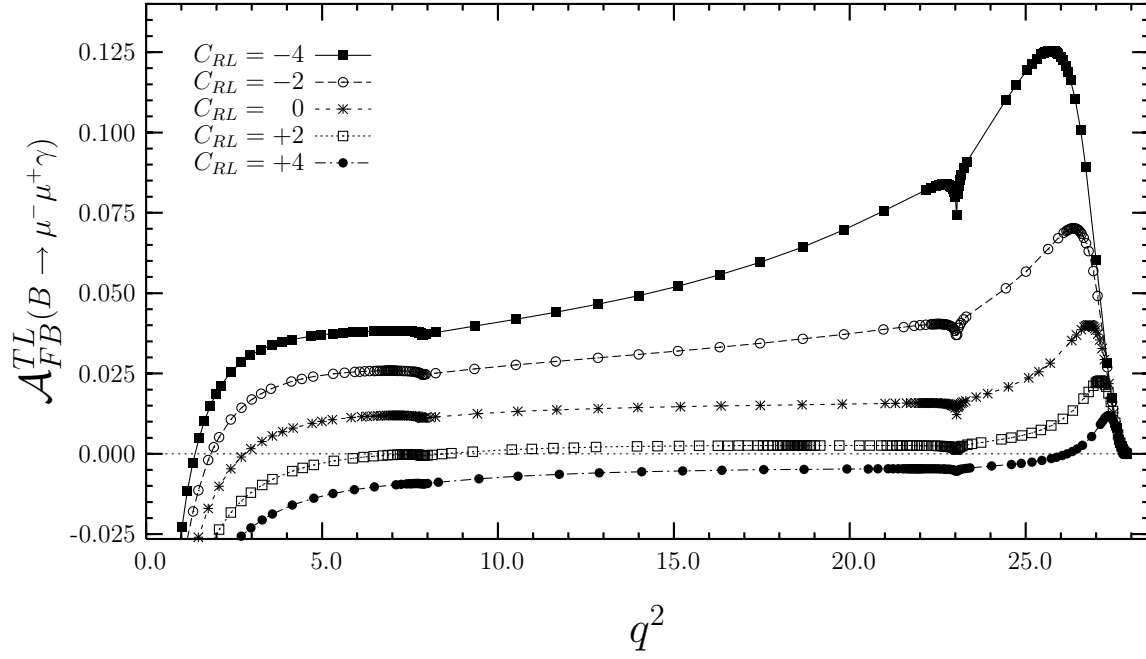


Figure 7:

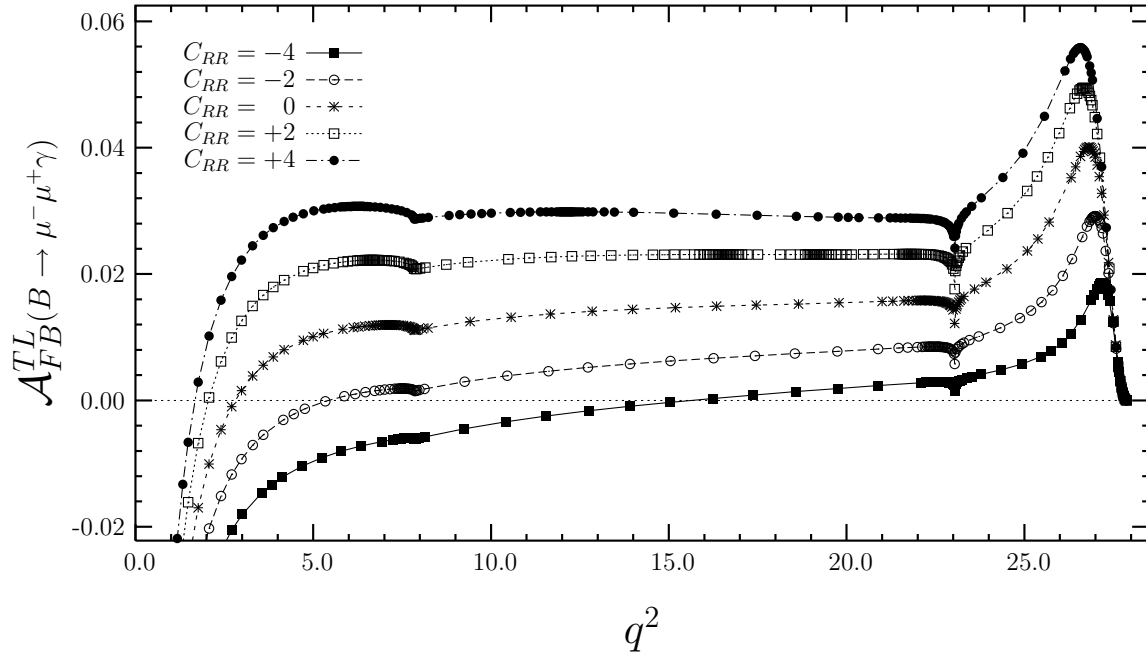


Figure 8:

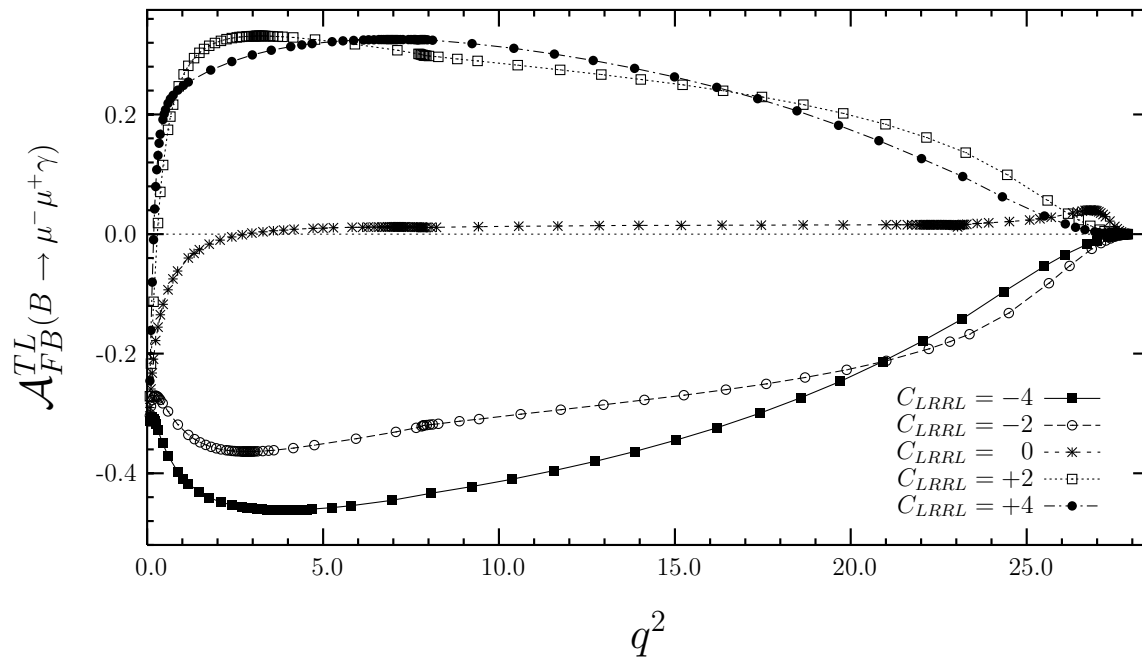


Figure 9:

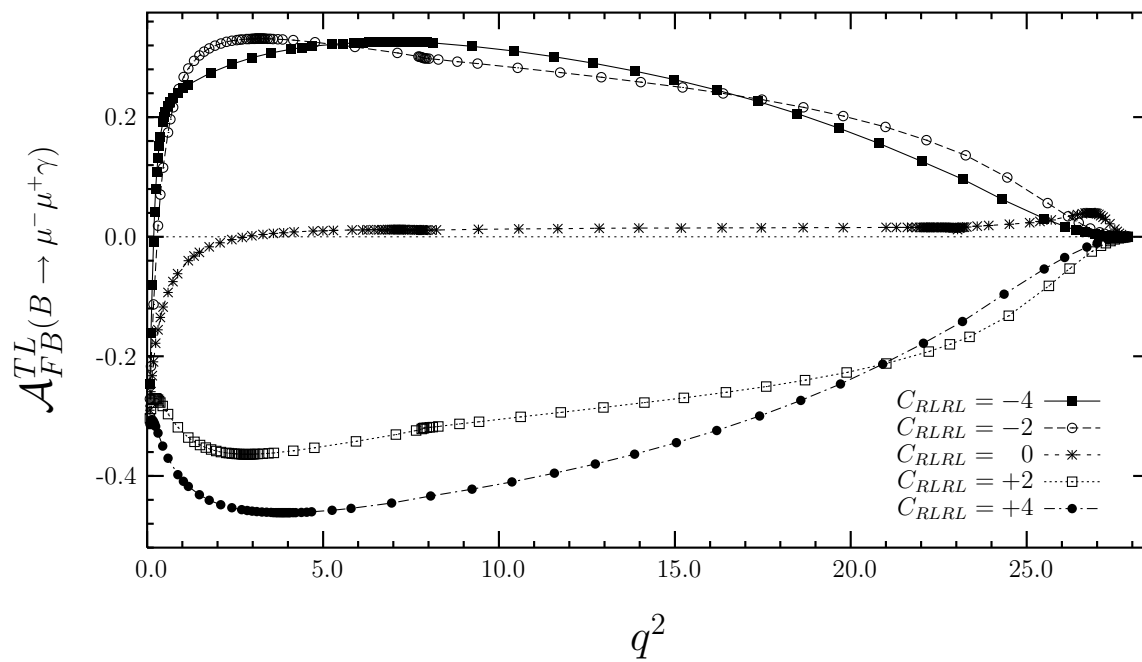


Figure 10:

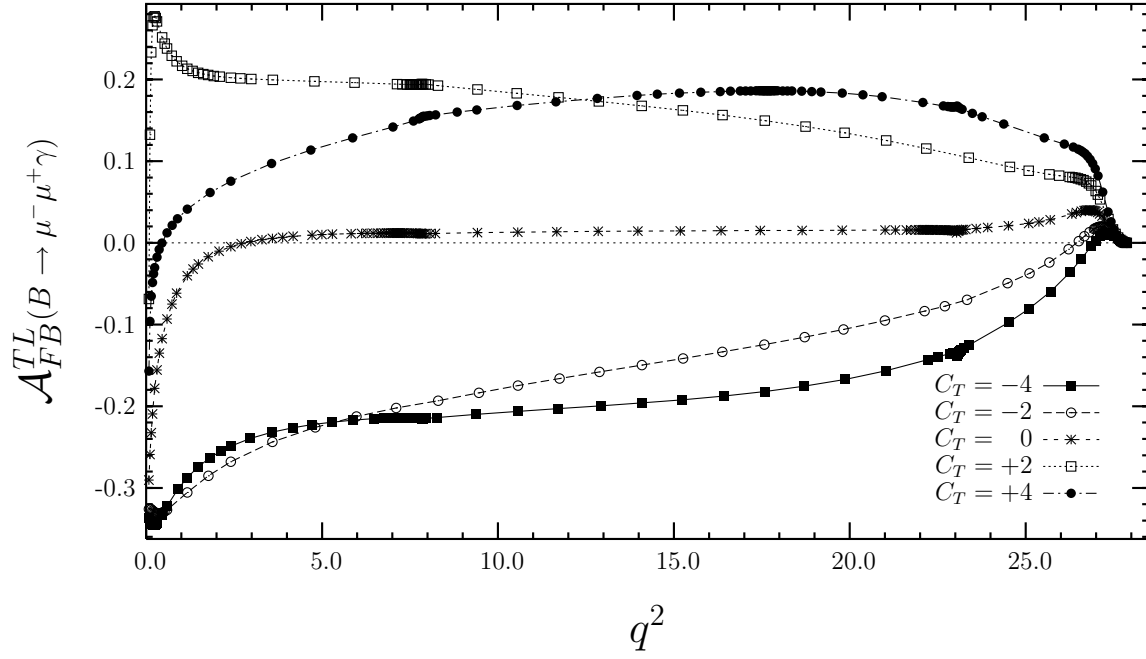


Figure 11:

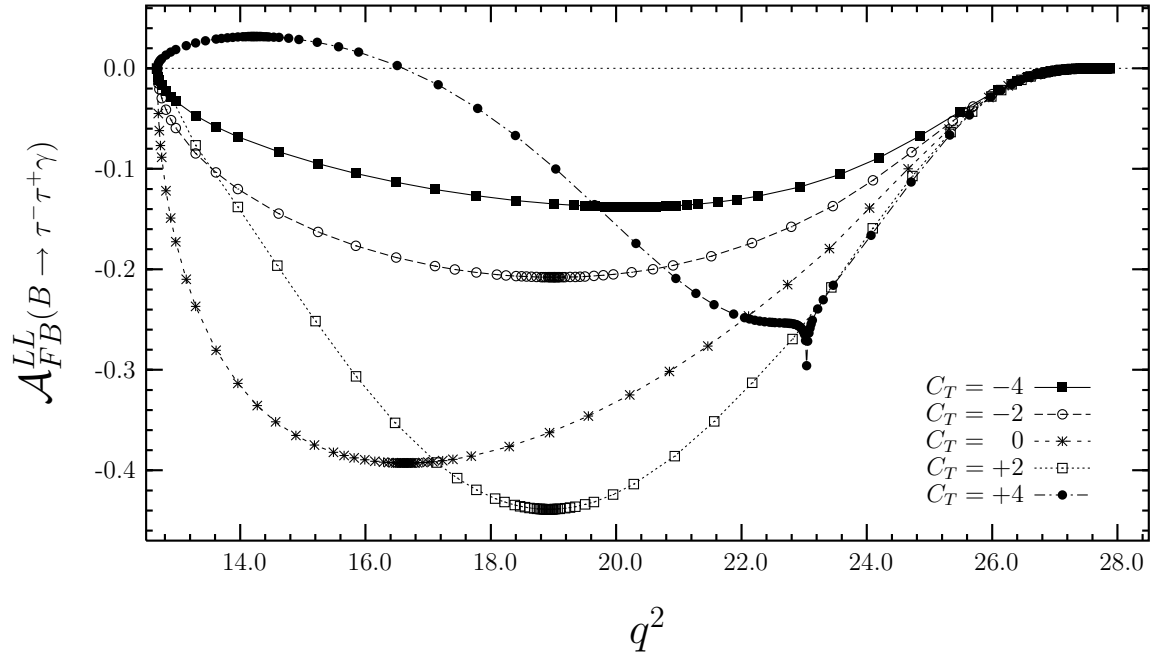


Figure 12:

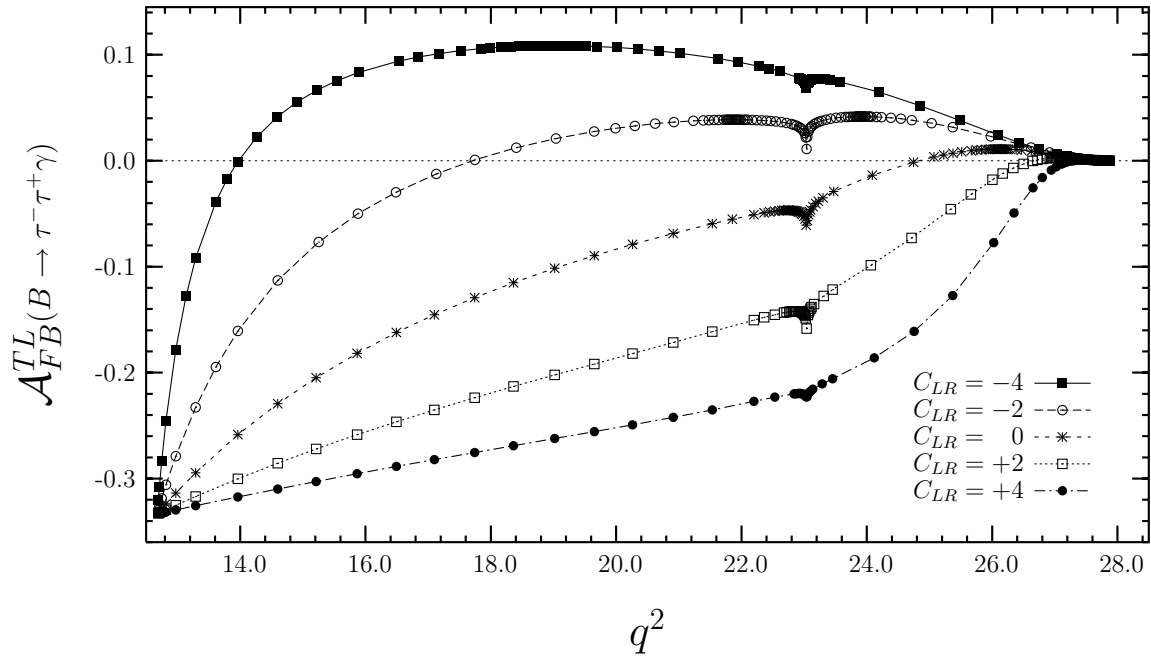


Figure 13:

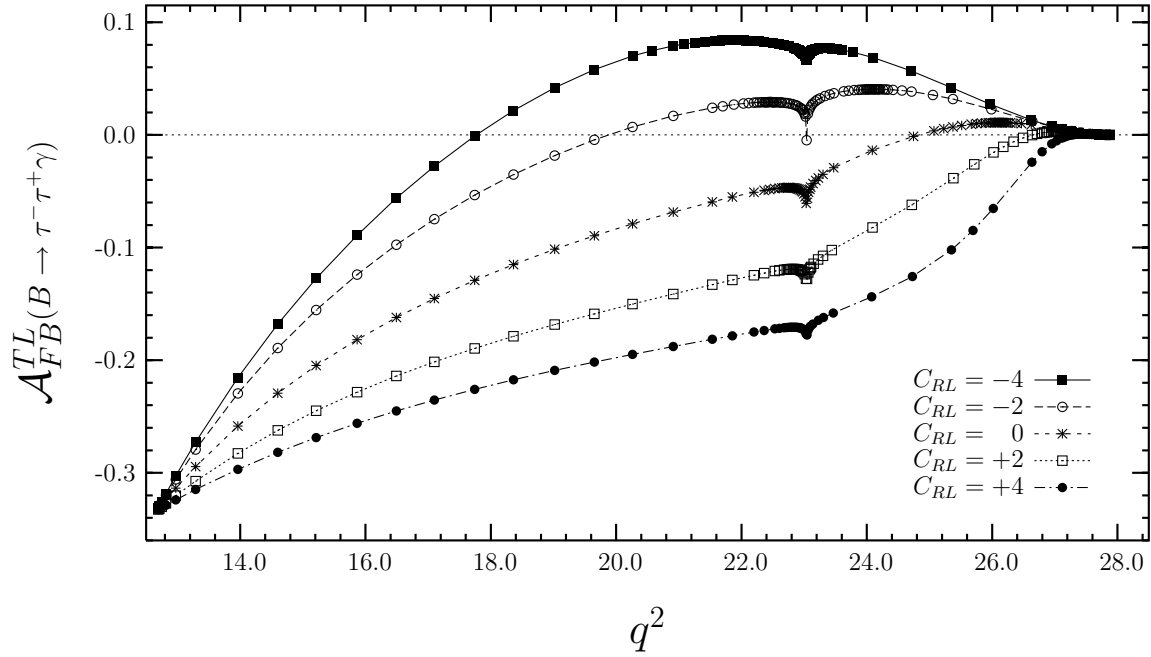


Figure 14:

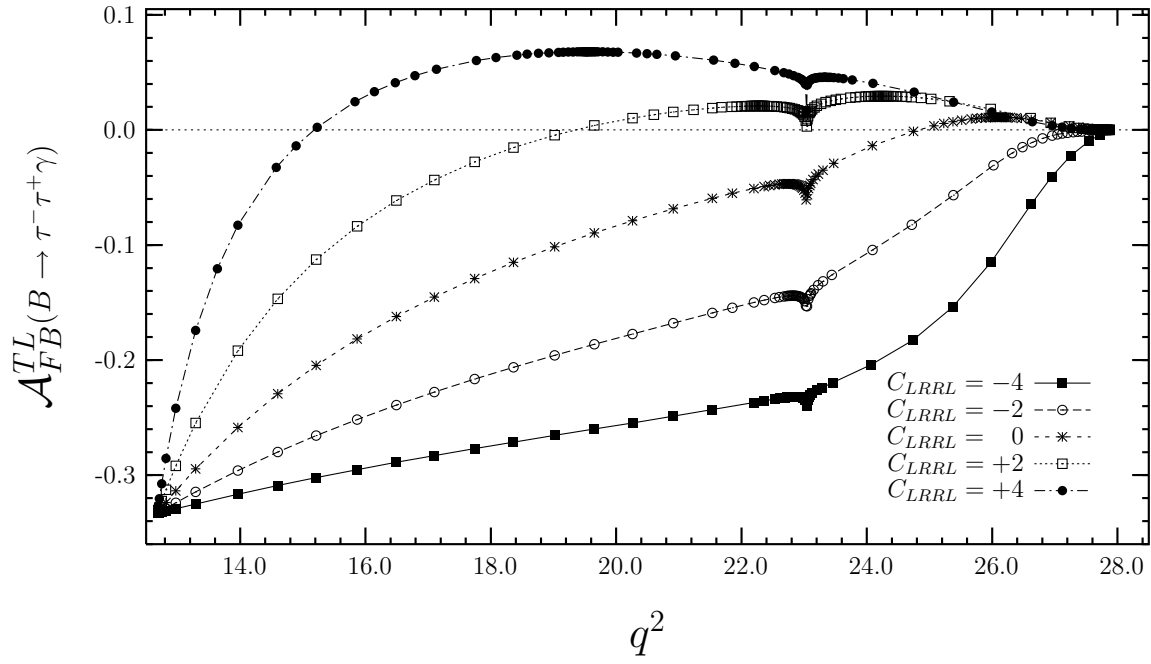


Figure 15:

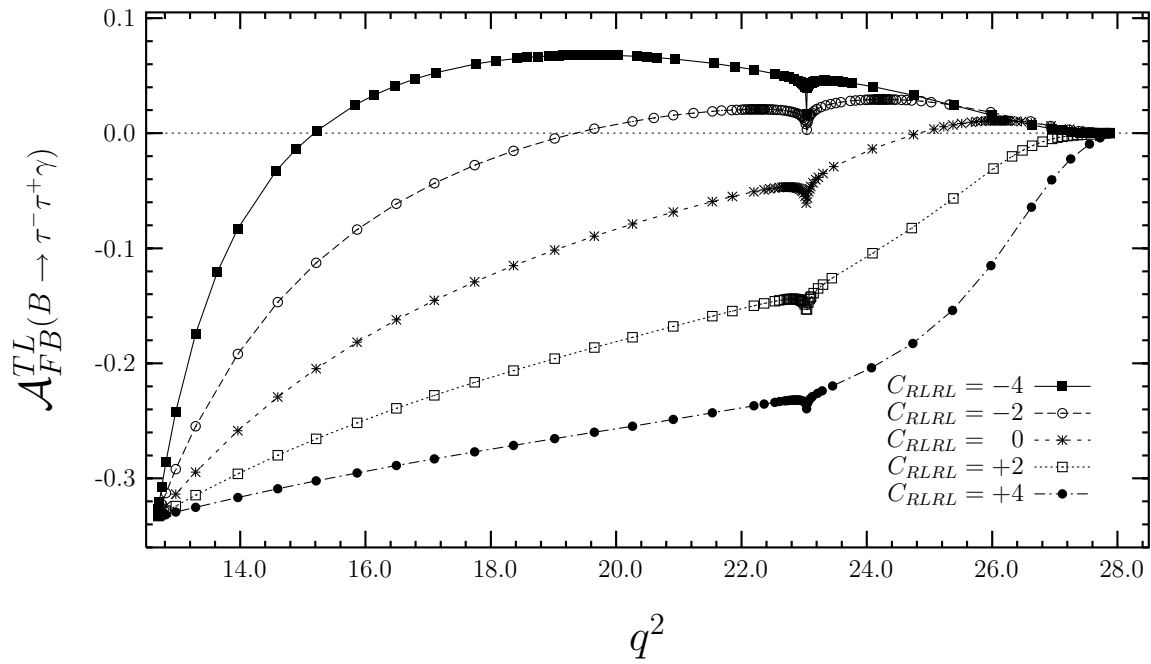


Figure 16:

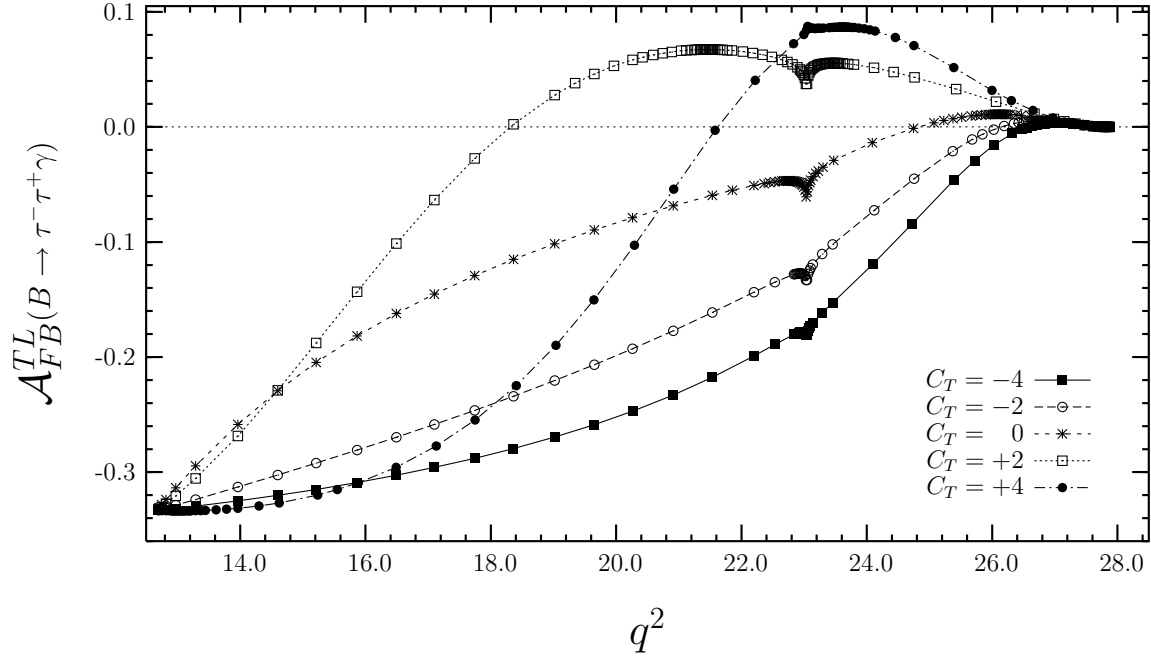


Figure 17:

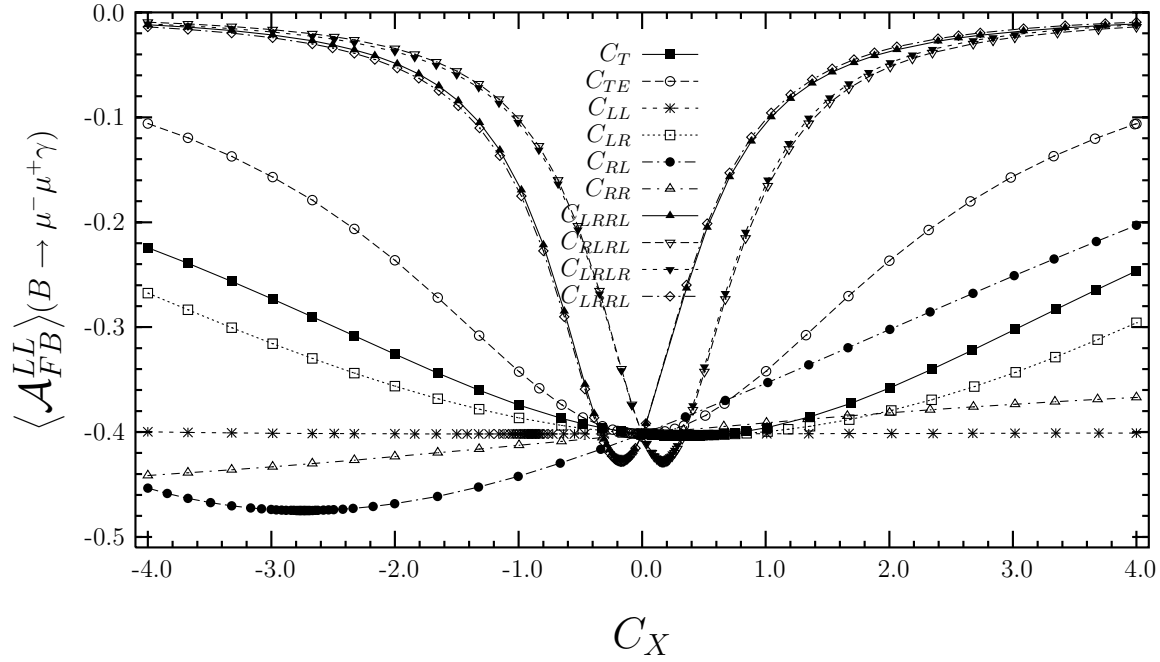


Figure 18:

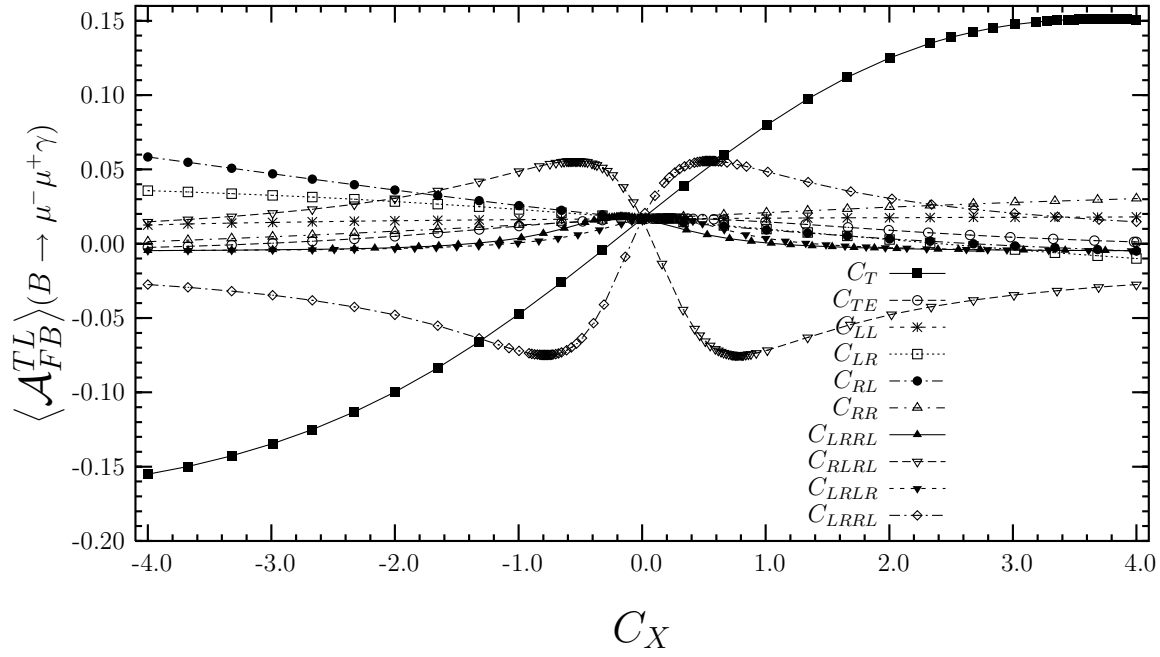


Figure 19:

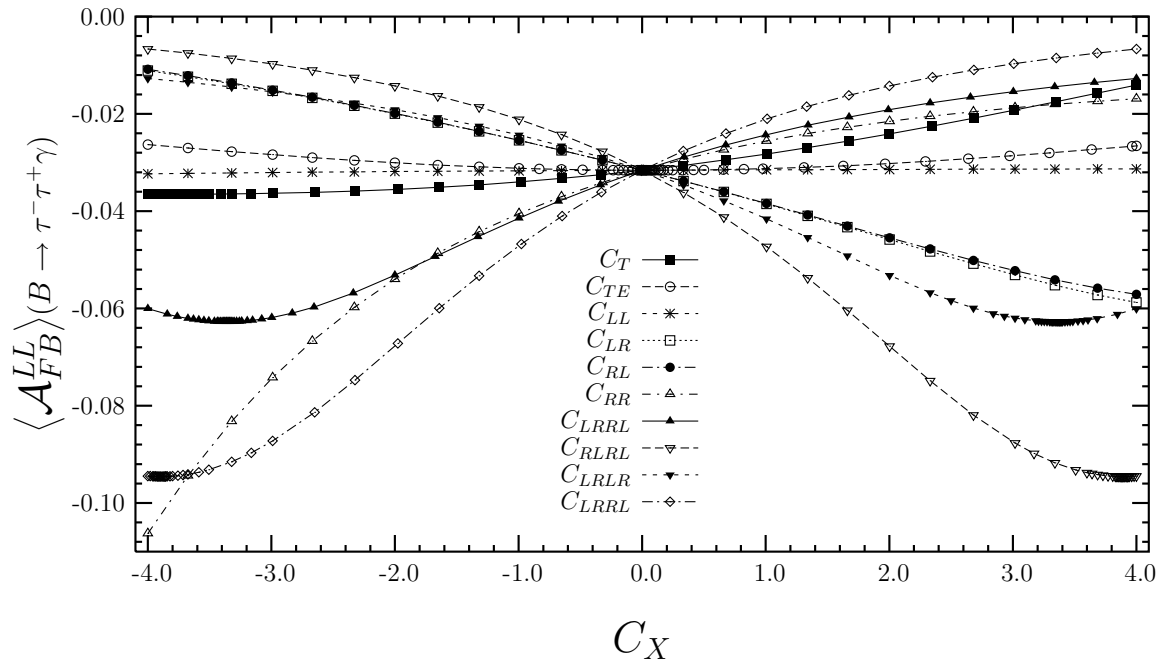


Figure 20:

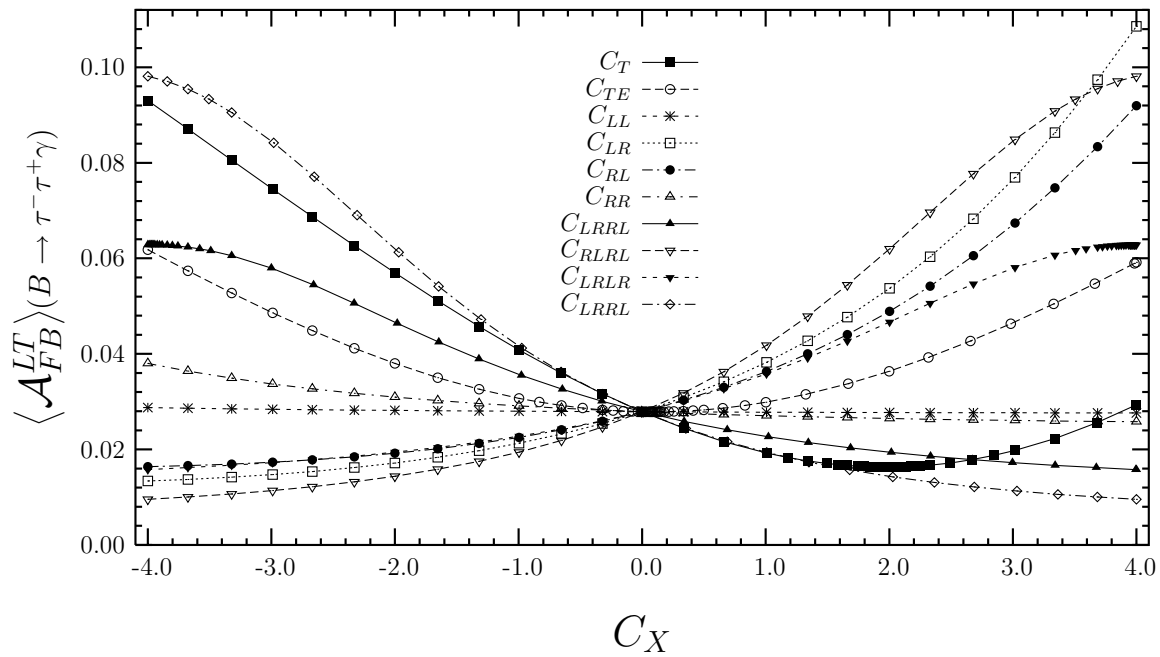


Figure 21:

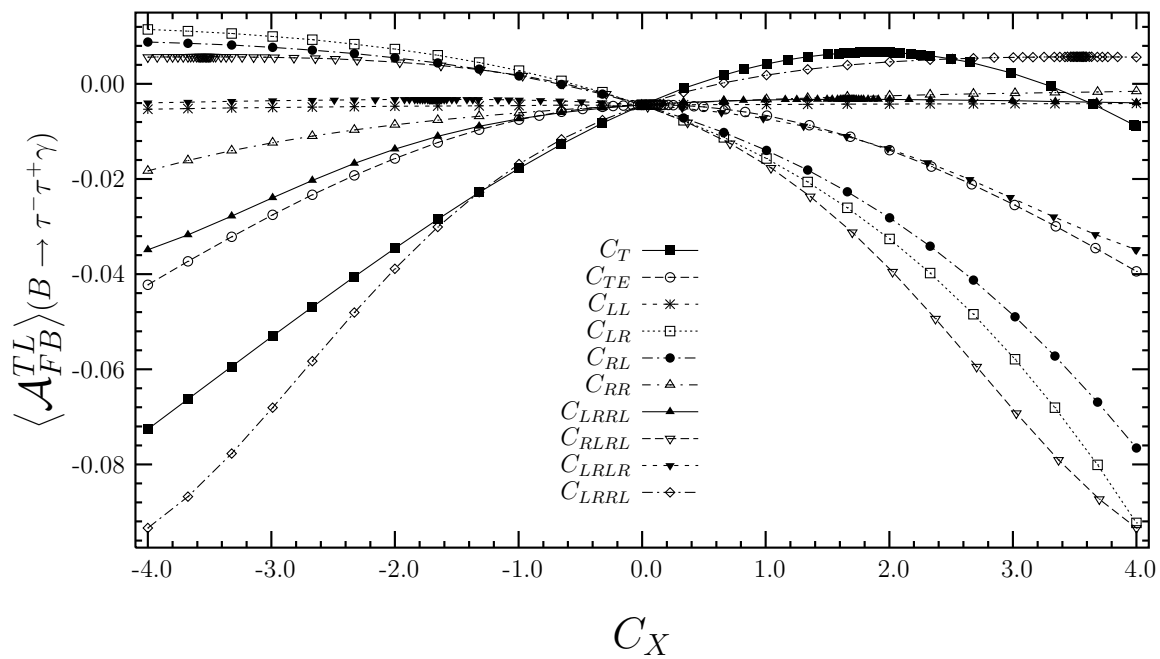


Figure 22: